INFORMATION TO USERS

This manuscript has been reproduced from the microfilm master. UMI films the text directly from the original or copy submitted. Thus, some thesis and dissertation copies are in typewriter face, while others may be from any type of computer printer.

The quality of this reproduction is dependent upon the quality of the copy submitted. Broken or indistinct print, colored or poor quality illustrations and photographs, print bleedthrough, substandard margins, and improper alignment can adversely affect reproduction.

In the unlikely event that the author did not send UMI a complete manuscript and there are missing pages, these will be noted. Also, if unauthorized copyright material had to be removed, a note will indicate the deletion.

Oversize materials (e.g., maps, drawings, charts) are reproduced by sectioning the original, beginning at the upper left-hand corner and continuing from left to right in equal sections with small overlaps.

Photographs included in the original manuscript have been reproduced xerographically in this copy. Higher quality 6" x 9" black and white photographic prints are available for any photographs or illustrations appearing in this copy for an additional charge. Contact UMI directly to order.

Bell & Howell Information and Learning
300 North Zeeb Road, Ann Arbor, MI 48106-1346 USA
800-521-0600

UMI®

Governor Control for Kakabeka Falls Generating Station

Robert E. Doan ©
September 1999

A Thesis submitted in partial fulfillment of the requirements of the Msc. Eng. Degree
in
Control Engineering
Faculty of Engineering
Lakehead University
Thunder Bay, Ontario

Abstract

This thesis examines a specific problem of governor control on a set of hydroelectric turbines that suffer from severe wicket gate leakage. Linear modeling and the steady state behavior of each turbine is investigated and used to determine the best means of speed control. Findings show that a secondary water control device may be used with the wicket gates to alleviate the effects of leakage while the generator is disconnected from the transmission system. The control method results in two distinct modes of turbine operation, with each having significantly different dynamic characteristics.

A digital speed droop governor scheme is considered in a gain scheduling arrangement to account for the two operating modes. The stability boundaries of the governor parameters are investigated, and an output feedback cost minimization algorithm is used for obtaining controller gains. An outline of the software used to implement the governor on an industrial programmable controller is presented, and the experimental performance for the turbines is compared to the theoretically developed model.

Table of Contents

List of Figures & Tables

Chapter 1

Station Overview

1.1 Introduction

Kakabeka Falls GS is a small hydro-electric generating station situated on the Kaministiquia river approximately 20km west of Thunder Bay, Ontario. The plant is owned and operated by Ontario Power Generation, and is one of the oldest stations of its type in the province. Construction of the plant began in the late 1800's and was complete by 1904, during the early stages of Ontario's electrification.

Although the plant is nearing its 100th year of service, frequent capital reinvestment has allowed the facility to keep pace with modern electrical generating stations. In 1998 a new plant automation system was installed, to facilitate remote control and monitoring. Before this time, many of the critical plant operations were done manually by a plant operator. With the newly installed equipment, Ontario Power Generation hoped to perform the following plant operations from its central operating & maintenance facility:

- Automatic unit start-up and shutdown of the generators.
- Automatic generator synchronisation to the power system.
- Automatic control of electrical power production and water usage.

The automation system installed at the plant is based on the Modicon "Quantum" family of programmable logic controllers (PLC). A system of this type was chosen because it is adaptable to many industrial applications, it can handle a large number of field wired I/O signals, and it allows the end user to tailor fit the software logic to specific design requirements.

This thesis deals primarily with one challenging aspect of the station automation: the design a digital governor control algorithm for implementation on the PLC. The success of the entire project hinged on the ability of the control system to provide adequate speed regulation of the generating units. Although this is a straightforward task at typical hydro

generating stations, problems unique to Kakabeka required further review of the feasibility and design of this control function.

In this chapter an overview of the plant equipment and operation is given, along with the conditions that make the task of speed governing at Kakabeka unique. In Chapter 2, a linear model is formulated for each of the plant generating units. Steady state turbine behavior is investigated and used to determine the best means of operation. The chosen feedback control structure used for speed governing is set out in Chapter 3. Tuning parameters are derived based upon the stability boundaries of the closed loop system, and the governor control algorithm and experimental data are presented, to support the theoretical development.

1.2 Plant Electrical System

Kakabeka Generating Station contains four horizontally mounted synchronous generators (see Figure 1-1) each connected to a Francis water-wheel turbine. Generators 1 through 3 are equivalent in size and rating, while generator 4 is slightly larger in capacity. Each of these units has a power transformer connected directly to the stator windings. The transformers are configured in a Delta Y-Ground arrangement and provide voltage step-up from 4kV at the generators, to the 25.0kV distribution bus. Power from the plant is transferred to the Ontario's bulk electrical system via two 25.0kV feeders.

A number of oil-filled circuit breakers provide switching and fault isolation for the generators and distribution feeders. The generator breakers are used primarily for synchronizing and removal of individual generating units from the power system. However, they also provide isolation in the event of an electrical fault. The line breakers are used to isolate the plant from the power system in the event of a feeder or station bus fault, and also serve as isolation points of electrical equipment when routine maintenance is performed. Fault detection on the various pieces of electrical apparatus is achieved with high-speed protective relaying schemes located within the plant.

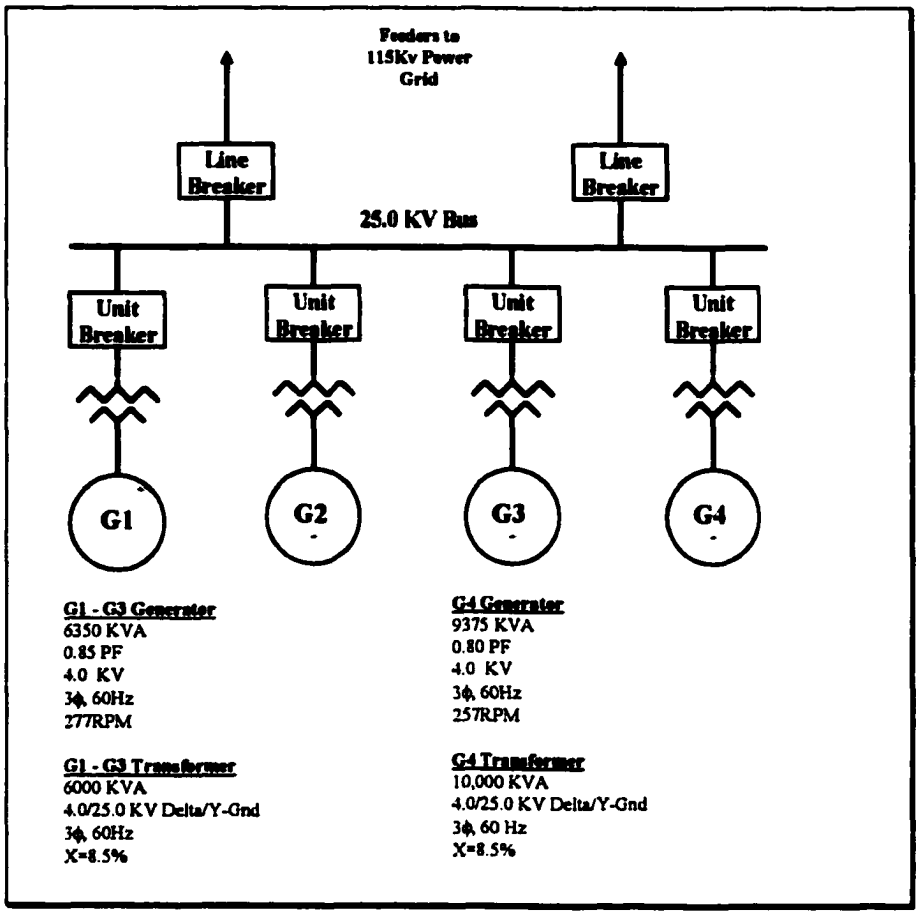

Figure 1-1 Kakabeka GS Electrical Overview

1.3 Water Conveyance System

Kakabeka generating station is a "run of the river" type hydro plant; A dam located in a section of the Kaministiquia River forms a small head pond to facilitate plant operation. The term "run of the river" is used because the plant water consumption must closely match river flows at all times, in order to maintain sufficient water level for operation.

The major element in the water conveyance system is a 2km long aqueduct, which is used to bridge most of the gap between the dam, and the powerhouse (See Figure 1-2). This single buried concrete pipe is 5 meters in diameter and can transport up to 54 cubic meters of water a second from the dam to the surge tank. The surge tank acts as a relief point in the water system, absorbing any pressure fluctuations resulting from changes in water flow. Four penstocks carry water from the surge tank to the water-wheel turbines located in the powerhouse. The penstocks are constructed of riveted steel and are supported by a number of concrete saddles at ground level. The fourth penstock is somewhat larger in diameter than the first three in order to meet the water requirements of the largest generating unit. The turbines are dual impeller Francis type units, all with horizontal drive shafts and horsepower ratings to match the coupled synchronous

machines. The turbines are physically mounted on top of the concrete foundation and have large exposed cast iron scroll cases that sit above the power house floor.

Three elements help to control the flow of water through the plant: The headgates located at the dam intake, the butterfly valves located in each penstock, and the turbine wicket gates. Both the headgates and the butterfly valves are operated with the aid of electric motors, while the wicket gates move with the aid of a high-pressure hydraulic oil system. During normal plant operation the butterfly valves remain fully open on all functioning generators; the only time these devices change position is during generator startup and shut down. The wicket gates are used to regulate generated power, and are used as the primary control element for speed regulation. At typical hydro plants headgates are normally used for water system isolation following a plant shut down; otherwise they remain fully open at all times. At Kakabeka, the head gates are used continuously to throttle or restrict the amount of water entering the Aqueduct. This operation is necessary because the maximum permissible water level in the surge tank is less than the nominal head pond level. Without the water losses introduced by the head gates, the plant surge tank can overfill and the excess water must be sent to the riverbed through an emergency spillway.

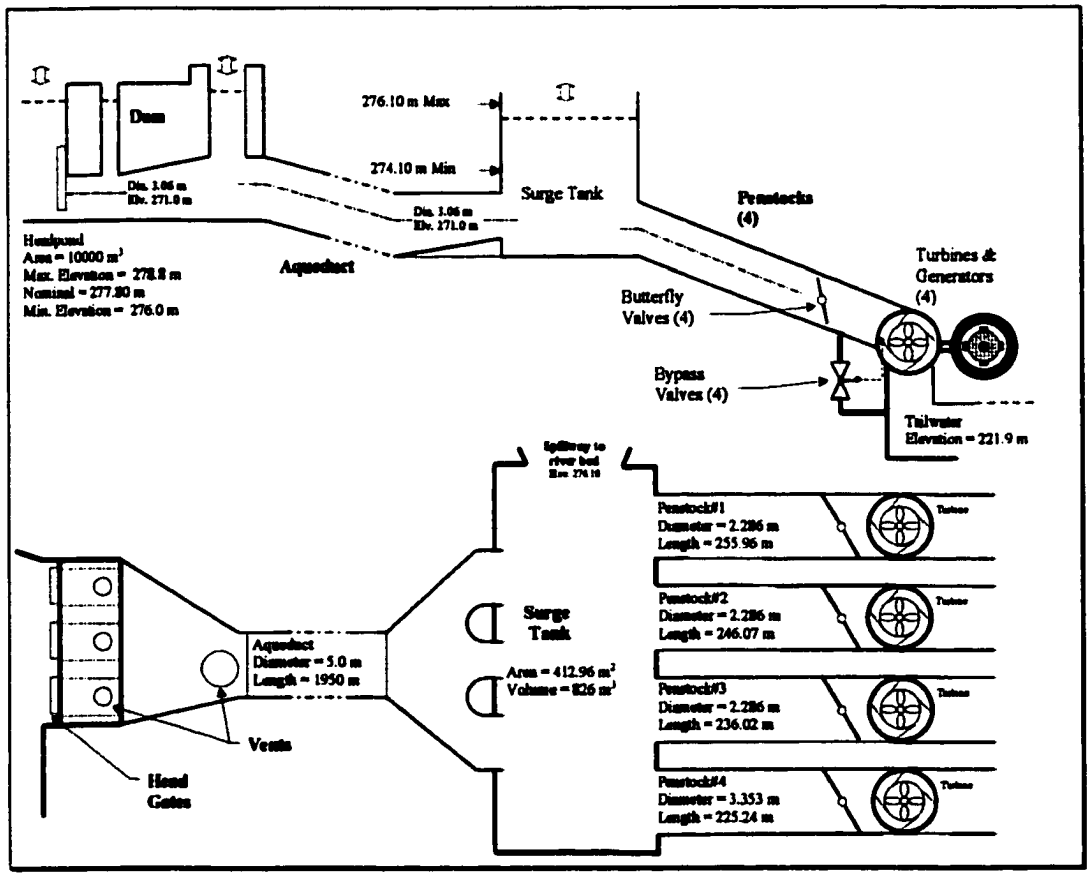

Figure 1-2 Water Conveyance System

A bypass valve on each unit is used to divert water from the base of the penstock to the draft tube. The purpose of these devices is to protect the turbine scroll case and penstock from damaging water hammer effects that can occur with rapid turbine shutdown. On generating units 1,2 and 3 these valves are mechanically coupled to the wicket gates and are forced open when the wicket gates approach there fully closed position. On generator 4 the bypass valve is connected to the wicket gates through a dashpot and spring mechanism. The bypass valve opens whenever the wicket gates move rapidly towards closure.

1.4 Plant Control and the need for Governing

Governor control systems installed on hydro electric generating units have three primary functions:

1. Speed regulation of the generator for synchronizing when the unit is disconnected from a power system.
2. Stable load regulation via the wicket gates, while the generator is connected to the power system.
3. Frequency stabilization during power system disturbances.

Electromechanical governor systems are common in older stations, while newer plants or refurbished plants are now using digital governor systems for better performance and reduced maintenance. In both cases, these systems use wicket gate position and speed sensing feedback signals to drive a wicket gate actuator, in order to maintain unit speed and load at some desired level. The actuators are typically high-pressure hydraulic systems utilizing electrically controlled pilot valves, however servomotors are also utilized on smaller units.

While synchronizing, the governor must be capable of matching the generator's speed to that of the power system so that the slip-rate between the two systems is minimized. With minimal slip, the timing for the generator breaker to close at a zero phase angle crossing becomes less critical, and the power that is transmitted or taken from the system when the rotor is pulled into synchronism is minimized. When the generator is connected to the power system, the governor normally provides a means of controlling the wicket gates so that the amount of generated power may be regulated. However, during power system disturbances the governor will readjust gate position in an effort to correct frequency error.

The dynamic modeling of hydro plants and design of governor systems has been studied a great deal, and for a long time. Many technical publications may be found which discuss the various aspects of this subject. The most notable work on modeling may be found in reference [2]. This paper gives a very detailed summary of the dynamic equations that may be used to model a hydro plant, and experimental test data is provided to assess the suitability of the models presented. More recently, IEEE committee reports given in references [3] and [4] summarize the generally accepted techniques for both modeling and governor control of hydroelectric generation. Likewise, many methods of control have been devised. Speed droop and PID type governor systems are commonly

used in hydro plants and are prevalent in literature [4, 5, 10]. More recent publications site methods such as gain scheduling [11], adaptive control [12, 13] as well as H_∞ control techniques [14] for governing hydro turbines.

Standard speed governing procedures are not directly applicable to the Kakabeka plant under all operating conditions because of severe wicket gate leakage. When the Kakabeka generating units are connected to the grid system, their behavior is not unlike units at other hydro plants, however, when they are disconnected from the power system in an off-line mode of operation, speed governing is hampered. The residual flow of water that occurs with the gates are fully closed, causes each unit to spin above rated speed if unsynchronized from the power system. The leakage problem is partially due to the design of the turbines and partially because of the age of the plant.

Each of the turbines is composed of twin scroll cases and runners with a common draft tube. The scroll cases are divided into two parts along the horizontal centerline. The bottom section of the scroll case is affixed to the concrete foundation of the plant atop of the penstock opening. The top section of the scroll case is joined to the bottom by means of large machine bolts. A T-shaped draft tube sits between each of the scroll cases, and is independently affixed to the concrete foundation. A set of head covers encloses the runners, and provides a seal between each of the scroll cases and the draft tube flanges.

The head covers partially support the wicket gates, and also house some components of the wicket gate assembly. Each gate is supported at one end by a stub shaft that passes through the head cover and at the other by a "blind end" bushing in the back of the scroll case. Each of the stub shafts is connected to a common actuator ring by a number of gate arms. The gates are set in motion by way of a hydraulic cylinder, which rotates the actuator ring (see Figure 1-3).

The relative position between the draft tube and the bottom of the scroll cases has shifted over time due to movements in the concrete foundation. As such, the alignment of the head covers between the draft tube and the bottom of each scroll case is poor. Some of the gates are "tipped" in relation to the blind end bushing of the scroll case, and the heel and toe clearances of the wicket gates are affected. Efforts made to improve alignment during turbine maintenance have proved fruitless, as it has been found that the scroll cases actually move slightly between the pressurized and non-pressurized state. Any adjustment made to the turbine assembly while in the de-watered state, change when the turbine is placed back in service.

To compound the alignment problem, the gate arms are not designed with any adjustable linkage or shear mechanism; the stub shafts are simply keyed to the gate arm. Quite often the gates are forced closed on debris from the riverbed that has found its way into the penstock. Force from the hydraulic cylinder causes the stub shafts to twist slightly, and over time repeated stress on the gate shafts results in poor gate shut off. The lack of adjustable gate linkage hampers any effort to make gate adjustments, except during major overhauls when re-keying of the gate stubs is possible.

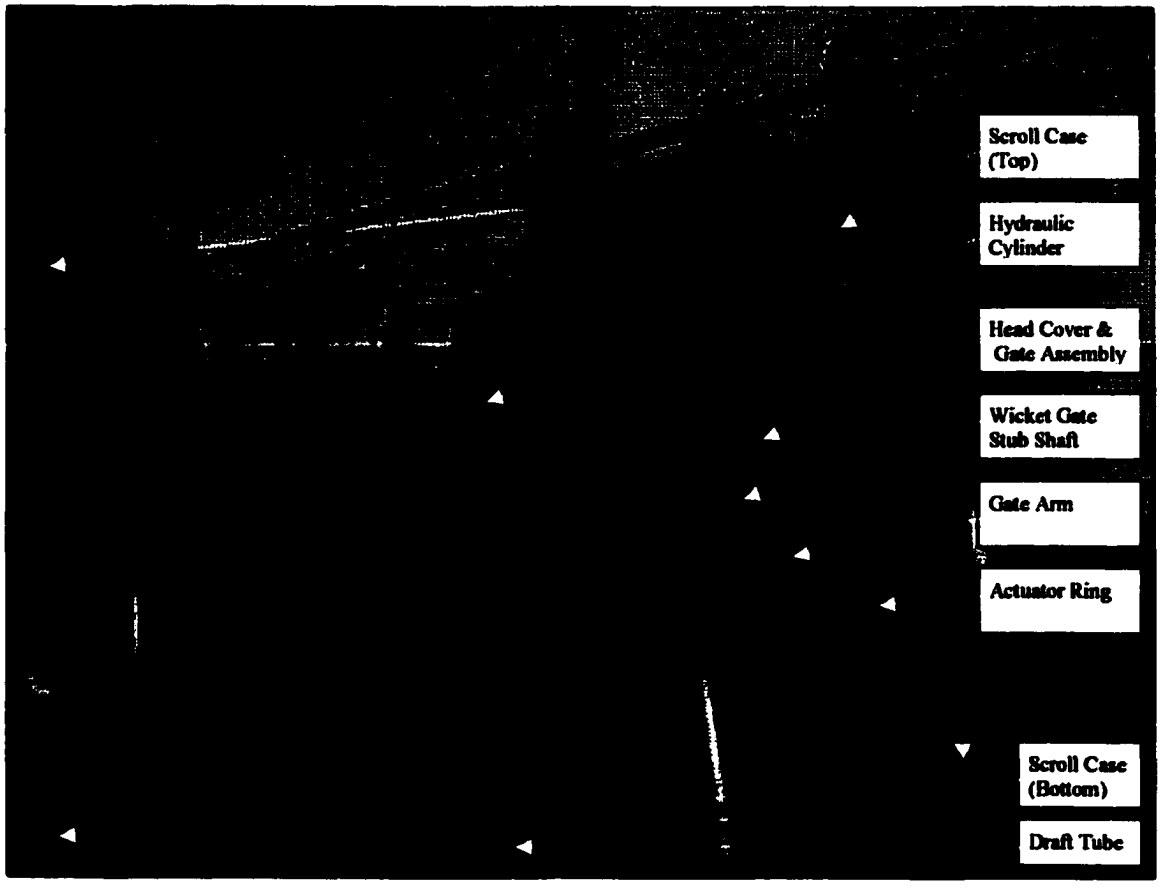

Figure 1-3 Turbine Assembly

The original mechanical governors installed during the plant's inception were removed from service in the 1980's when the leakage problem made off-line speed governing of the generators impossible. At the time, Ontario Power Generation (then Ontario Hydro) decided that it would be prohibitively expensive to refurbish and align bore all of the wicket gates as well as change the linkage design. From then on, a somewhat unconventional operating procedure was adopted.

The penstock butterfly valve upstream of each turbine was used as a throttling device during unit startup. A plant operator would manually adjust both the butterfly valve position and wicket gate position to achieve synchronous speed. With the aid of a synchroscope, the plant operator would close the unit breaker and then completely open the butterfly valve. The butterfly valve throttling effectively reduced the available head at the turbine so that lower unit speeds were achievable. Although motorized, the butterfly valve could not completely replace the function of the wicket gates because of its slow operating speed.

Under normal operation, the large power system to which Kakabeka was connected would regulate each turbine's speed while online: The wicket gates were used strictly for

the control of generated power. The risk however was that a system disturbance might create an islanding condition, leaving Kakabeka connected to an isolated customer load. The lack of speed governing would result in a dangerous over-speed condition and possible customer equipment damage. To circumvent this problem additional over and under speed protection was installed at the plant, so that the generators would be shut down and isolated from the power system during minor frequency disturbances. Although the scheme provided adequate speed protection and it allowed the generators to function in the same manner as other plants, the units were not able to contribute to power system stability during load disturbances. Furthermore, the plant often required time consuming generator restarts when these events occurred.

1.5 Problem Statement

At present, the turbines are at the halfway point in a planned major maintenance cycle of 30 years. It is likely that that the issue of wicket gate refurbishment will be revisited, however this will not be for some time to come. The costs associated with turbine refurbishment are also far beyond the budgeted dollars for the plant automation project.

The challenge at hand is to utilize the newly installed plant programmable controller to achieve automatic startup and synchronization of the generating units. The "automatic" control strategy implemented will have to be similar to the one previously used because of the gate leakage; both the wicket gates and butterfly valve will have to be operated to accomplish off-line speed regulation. Startups must be fast so that extra generation may be called upon in a minimal amount of time, and the off-line speed regulation must be good so that synchronization is smooth and non-impactive to the generator or the power system. Any closed loop control that is used must be simple and robust so that technical support staff can comprehend and maintain the system, but will not be unduly burdened with frequent "tuning".

Further improvements that are to be considered in the design are a limited degree of on-line speed regulation. Although the gate leakage makes it impossible to achieve speed control in the event of a full load rejection, and the over speed protection described above will still be required, less severe power system disturbances should be matched with an appropriate amount of prime mover power. In this way the plant as a whole will contribute positively to the overall power system stability.

Chapter 2

Linear Modeling of Hydro Generators

2.1 Introduction

In this chapter a linear model will be formulated for the Kakabeka Generating Units. The model will be based on the generally accepted techniques found in various references [2, 3, 4, 5, 7]. Any assumptions made in formulating or simplifying the model are stated, along with the circumstances under which the assumptions are valid.

The steady-state turbine behavior will be used to assess how the wicket gates and the butterfly valve should best be used for speed regulation off-line. Stable operating points will be selected for the off-line and on-line modes of operation to determine the values of the parameters in the linear model.

Unless otherwise stated, upper case variables will represent quantities in engineering units, and lower case variables will represent deviations from a steady state operating point in per unit form. Variables that define a steady state operating point will be denoted with a subscript '$\bullet$', and per-unit base quantities will be denoted with a subscript 'o'.

2.2 Penstock Water Modeling

The modeling of any hydro generating system begins with the study of water flow in the penstock, and the basis of a water model stems from a set of partial differential equations derived in many elementary fluid mechanics textbooks [1].

$$\frac{\partial V}{\partial x} = -a\frac{\partial H}{\partial t} \tag{2.1}$$

$$\frac{\partial V}{\partial t} = -g\frac{\partial H}{\partial x} \tag{2.2}$$

$$\alpha = \rho g \cdot (\frac{1}{K} + \frac{D}{eE})$$

With the variables defined as:

V – fluid velocity (m/s)
H – Pressure head (m of water)
ρ – Fluid density (Kg/m^3)
g – Gravitational constant (9.81 N/Kg)
D – Inside pipe diameter (m)
e– Pipe wall thickness (m)
E – Young's modulus for the pipe material (N/m^2)
K – Bulk modulus of elasticity of the fluid (N/m^2)
x– linear displacement along the pipe axis (m)
t– Time (s)

These equations describe the flow of a compressible liquid through an elastic pipe, with head loss due to friction neglected. In [1] a numerical method is given for performing time domain simulations of fluid flow.

In [2] it is shown that Equations (2.1) and (2.2) may be approximated by:

$$H_2(s) = \operatorname{sech}(T_e s) \cdot H_1(s) - Z \cdot \tanh(T_e s) \cdot Q_2(s) \qquad (2.3)$$

$$Q_1(s) = \cosh(T_e s) \cdot Q_2(s) + \frac{1}{Z} \cdot \sinh(T_e s) \cdot H_2(s) \qquad (2.4)$$

$$T_e = L \cdot \sqrt{\alpha / g}$$

$$Z = \frac{1}{\sqrt{\alpha \cdot g} \cdot A}$$

with assumptions on the initial conditions, and some partial derivatives taken as full derivatives.

The subscripts on Q and H represent some fixed distance along a pipe axis. However, in the case of a penstock where the point of interest is the turbine, H_2 and Q_2 may be taken as the head and flow at the turbine, while H_1 and Q_1 may be taken as the head and flow at the surge tank or water reservoir. L is the axial distance along the penstock between the turbine and the water source and A is the internal cross section area of the penstock. T_e is defined as the pipe elastic time and Z is defined as the pipe impedance. s is the Laplace transform operator.

In [2] it is also shown that Equation (2.3) and (2.4) may be rewritten in variable sets of per-unit deviations from some nominal head H_0 and flow Q_0 as follows:

$$h_2(s) = \operatorname{sech}(T_e s) \cdot h_1(s) - Z_0 \cdot \tanh(T_e s) \cdot q_2(s) - k \cdot q_2(s) \qquad (2.5)$$

$$q_1(s) = \cosh(T_e s)\cdot q_2(s) + \frac{1}{Z_0}\cdot \sinh(T_e s)\cdot h_2(s) \qquad (2.6)$$

$$Z_0 = \frac{Z\cdot Q_0}{H_0}$$

$$k = 2\cdot c\cdot |Q_2|$$

Equation (2.5) also incorporates a head loss term k that may be used to account for minor water losses in the penstock. The loss is assumed to be of the form $H_l = c\,Q\cdot|Q|$, which is standard for turbulent fluid flow in a pipe. The proportionality constant c may be computed using the Darcy-Weisbach equation [1], or determined experimentally.

If the head in the surge tank or water reservoir is assumed to remain relatively constant ($h_1=0$) then Equation (2.5) may be rewritten as:

$$\frac{h_2(s)}{q_2(s)} = -Z_0\cdot\tanh(T_e s) - k \qquad (2.7)$$

This assumption is valid for most hydro plants with an appropriately sized surge tank, or a penstock that is directly connected to a large water reservoir. The transfer function of (2.7) encompasses the effects of pipe elasticity and water compressibility, which are significant with a long penstock and/or a high head plant. References to Equation (2.7) are common, and may be found in [2,4,5,6].

The hyperbolic term in (2.7) may be eliminated using a number of approximations so that the transfer function is of linear form for applications requiring control design [2,5,6]. The complexity of the approximation depends on the degree to which pipe elasticity and water compressibility are considered significant. A simple first order approximation suggested in [2] and [5] is

$$\tanh(x) \approx x \qquad (2.8)$$

which, when substituted into (2.7), produces an interesting result. This has been noted in [5] but is included here for clarity.

$$\frac{h_2(s)}{q_2(s)} = -Z_0\cdot T_e s - k$$

$$h_2(s) = -Z_0\cdot T_e s\cdot q_2(s) - k\cdot q_2(s)$$

$$\frac{dq_2(t)}{dt} = \frac{-1}{Z_0 T_e}(h_2(t) + k\cdot q_2(t))$$

$$\frac{dq_2(t)}{dt} = \frac{-H_0}{Q_0}\cdot\frac{gA}{L}(h_2(t) + k\cdot q_2(t)) \qquad (2.9)$$

Equation (2.9) is Euler's Equation for fluid flow in a pipe where the fluid is considered incompressible and the pipe walls inelastic [1]. The first order approximation has eliminated the traveling wave characteristics inherent to Equation (2.7)

For low to medium head applications, such as the Kakabeka plant, a first order approximation like that of (2.8) are generally acceptable [4], with Equation (2.9) more commonly stated as

$$\frac{h_t(s)}{q(s)} = -(\tau_w s + k) \tag{2.10}$$

$$\tau_w = \frac{Q_0 \cdot L}{g \cdot A \cdot H_0} \tag{2.11}$$

The time constant τ_w is commonly referred to as the water starting time.

Often the effects of water losses are insignificant, and k is assumed to be zero. In the case of the Kakabeka Plant, water losses in the penstock may be neglected under normal operating conditions, but water losses incurred while the butterfly valve is at fixed partial opening during generator startup and synchronization can not be neglected. The water losses in this mode of operation are consequential and must be included in the penstock water model. The butterfly valve may be treated as a linear valve as opposed to an equal percentage valve, because it will remain in a fixed position, and because the range of positional movement that will be studied is small. The standard equation used to describe the head loss across a linear valve may be found in [8], as well as many fluid dynamics textbooks such as [1]:

$$Q = C_b g_b \cdot \sqrt{H_b} \tag{2.12}$$

The fluid flow Q is considered to be proportional to the valve coefficient C_b, valve actuator position g_b, and the square root of the valve head loss H_b. To determine a value for the water loss constant k in Equation (2.10), one may linearize Equation (2.12) with respect to Q, at an appropriate operating point [15].

$$k = \frac{\partial H_b}{\partial Q} \cdot \frac{Q_0}{H_0}\bigg|_{Q_0, g_{b0}}$$

$$k = \frac{2Q}{(C_b g_b)^2} \cdot \frac{Q_0}{H_0}\bigg|_{Q_0, g_{b0}} \tag{2.13}$$

2.3 Turbine Modeling

The behavior of a hydraulic turbine is nonlinear in nature, with water head h, speed w, and wicket gate position g_t all acting on the primary variables of flow q and mechanical torque m.

The linearized small signal model most often used to characterize turbine behavior for governor design is [2,5]:

$$q = a_{11}h + a_{12}w + a_{13}g_t \tag{2.14}$$

$$m = a_{21}h + a_{22}w + a_{23}g_t \tag{2.15}$$

$$a_{11} = \frac{\partial q}{\partial h}, a_{12} = \frac{\partial q}{\partial w}, a_{13} = \frac{\partial q}{\partial g_t}$$

$$a_{21} = \frac{\partial m}{\partial h}, a_{22} = \frac{\partial m}{\partial w}, a_{23} = \frac{\partial m}{\partial g_t}$$

The partial derivatives a_{1i} and a_{2i} are dependent on the turbine operating point, and may be extracted from manufacturer's performance curves if such information is available. When not available, it is customary to linearize the equations for an ideal turbine to fit the small signal model of (2.14) and (2.15). No turbine information for the Kakabeka units was available and so the traditional ideal turbine model was adopted:

$$M = \gamma\rho g \cdot \frac{H_t \cdot Q}{W} \tag{2.16}$$

$$Q = C_t g_t \sqrt{H_t} \tag{2.17}$$

Equation (2.16) essentially states that the turbine converts water power $\rho g \cdot H_t \cdot Q$ to mechanical power $M \cdot W$ with an efficiency of γ. H_t is the turbine water head, Q is volume of water flow, M is the turbine torque, W the rotational speed, ρ is the water density and g is the gravitational constant. All variables are shown in upper case to denote that they are in engineering quantities, and not per-unit quantities.

Equation (2.17) is not unlike (2.12) in that it describes the relationship between water flow Q and turbine head H_t for a given wicket gate position. Since the wicket gates operate in a manner that is consistent with a linear valve, it is reasonable to assume that this relationship may be considered valid over most of the operating range of the gates.

Under the assumption that the turbine is operating at rated speed and that small changes in rotational speed have little effect on water flow, the partial derivatives of Equations (2.14) and (2.15) may be obtained by linearizing (2.16) and (2.17) about a steady state operating point [15].

$$a_{11} = \frac{1}{2}\frac{(C_t \cdot g_t)}{\sqrt{H_t}} \cdot \frac{H_0}{Q_0}\Bigg|_{H_{t0}, W_0, g_{t0}}$$

$$a_{12} = 0$$

$$a_{13} = C_t\sqrt{H_t} \cdot \frac{1}{Q_0}\Bigg|_{H_{t0}, W_0, g_{t0}}$$

$$a_{21} = \frac{3}{2}\gamma\rho g \cdot \frac{C_t g_t \sqrt{H_t}}{W} \cdot \frac{H_0}{M_0}\Bigg|_{H_{t0}, W_0, g_{t0}}$$

$$a_{22} = -\gamma\rho g \cdot \frac{C_t g_t H_t^{3/2}}{W^2} \cdot \frac{W_0}{M_0}\Bigg|_{H_{t0}, W_0, g_{t0}}$$

$$a_{23} = \gamma\rho g \cdot \frac{C_t H_t^{3/2}}{W} \cdot \frac{1}{M_0}\Bigg|_{H_{t0}, W_0, g_{t0}}$$

The numerical values of these constants will be discussed in Section 2.6. However, it is important to note here that when the operating point and the per-unit base quantities are both chosen the same, the turbine constants of $a_{11}=0.5$, $a_{12}=0$, $a_{13}=1$, $a_{21}=1.5$, $a_{22}=-1$ and $a_{23}=1$ result. In many instances in the literature the assumption is also made that deviations in speed from the steady state operating point tend to be small, so that the interaction between torque and speed is negligible ($a_{22}=0$). This is valid principally when the generator is connected to a power grid, since generator protection systems often incorporate under and over speed tripping elements, which only allow the turbine to operate within a narrow speed range (typically ± 10%). It is also worth noting that with these turbine parameters, and the penstock water dynamics of Equation (2.10), one may derive the classical water hammer formula often applied in hydro governing studies [2,3,4,5].

2.4 Wicket Gate Actuator Modeling

Considerable force is required to move the turbine wicket gates, and so each turbine has a hydraulic cylinder, pump and reservoir to provide gate movement. The cylinder is mechanically coupled to the wicket gates, and forces the gates open or closed with linear shaft motion. The rate of flow of hydraulic fluid to and from the cylinder determines the rate at which the gates move and is regulated by an electrically controlled proportional valve. The proportional valve accepts a 4-20mA signal, and regulates the oil flow rate to

the cylinder based upon the value of the input. Although the proportional valve does exhibit some dynamic properties of its own, the dominant dynamics occur at the hydraulic cylinder where fluid flow produces a rate of change in the observed wicket gate position.

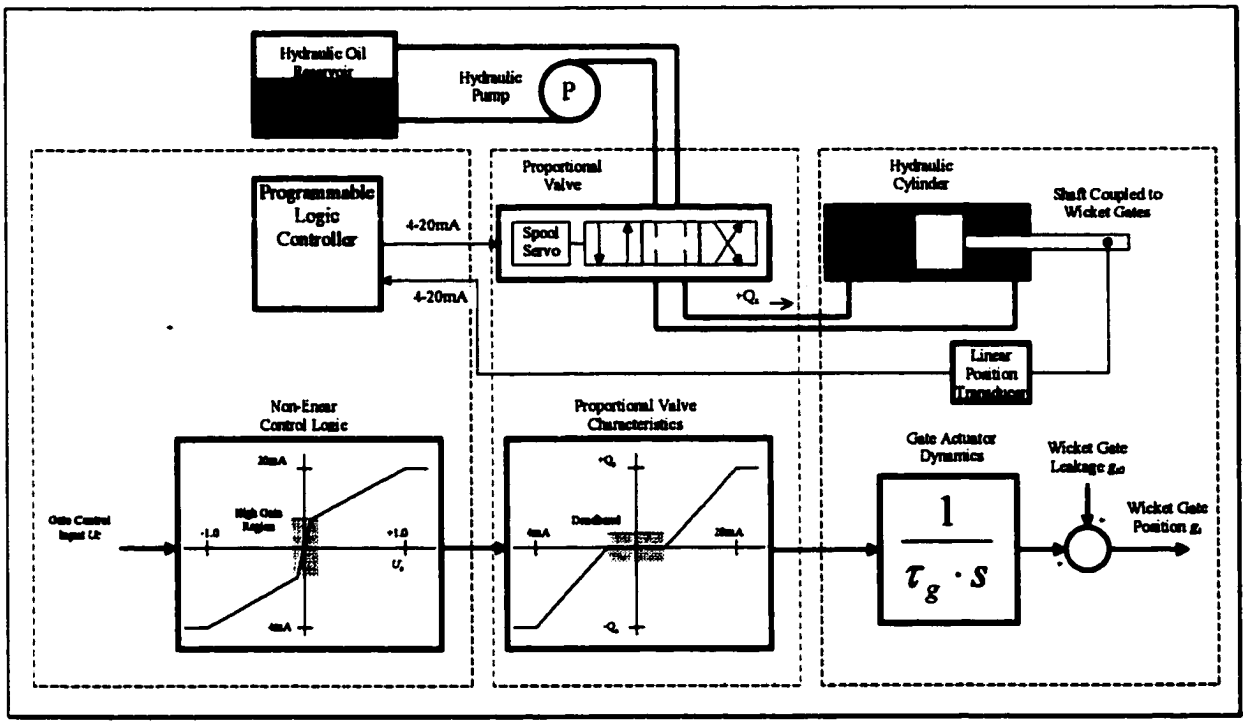

Figure 2-1 Wicket Gate actuator Dynamics

The force-mass dynamics of the proportional valve spool movement is low pass in nature but has a time constant that is insignificant when compared to the time constant of the hydraulic cylinder: For this reason it has been neglected from the actuator model. Likewise, the pump dynamics have been neglected as testing has shown the supply side pressure at the proportional valve only deviates a small amount when the wicket gates are operated in an aggressive manner.

The deadband present in the proportional valve spool at the neutral position was found to be significant, so to cancel its adverse effects a nonlinear element was introduced into the PLC software. In software, a high gain was applied to the valve-input signal within the region of the deadband, while an effective gain of unity was applied to the signal elsewhere.

The dynamic model shown in Figure 2.1 was derived from the following equations, taking into account wicket gate leakage.

$$g'_t(s) = \frac{1}{T_g \cdot s} \cdot u_c(s) \qquad (2.18)$$

$$g_t = g_t'\cdot(1.0 - g_{t0}) + g_{t0} \qquad (2.19)$$

$$0 \le g_t \le 1.0$$
$$0 \le g_{t0} \le 1.0$$
$$0 \le g_t' \le 1.0$$
$$-1.0 \le u_c \le +1.0$$

Equation (2.18) is the transfer function from the gate control signal u_c through to the observed wicket gate position g_t'. T_g is the time for the gates to move from the fully closed position $g_t'=0.0$, to the fully open position $g_t'=1.0$, with a control signal of unity applied. Equation (2.19) describes the actual turbine gate position, and is the sum of the wicket gate leakage g_{t0} and the observed gate position, scaled to adhere to the limits given above.

The small signal model for the above, given a per-unit base of unity and assuming operation about a stable operating point is:

$$g_t(s) = \frac{1}{\tau_g \cdot s} \cdot u_c(s) \qquad (2.20)$$

$$\tau_g = \frac{T_g}{(1 - g_{t0})}$$

2.5 Generator Modeling

A simple mechanical model is usually sufficient to account for generator dynamics when considering governor design [2,4,9]. This is because the most severe of speed disturbances often come in the wake of a generator breaker trip, when the electrical system is separated from the generator stator. All power once being transferred into the connected electrical system is now directed towards accelerating the generator rotor, and the governor is called upon to reduce turbine power before dangerous over-speeds occur. So too one may argue that load changes made to a single generating unit connected to an electrical system with large amounts of generation and load will have little effect on the system frequency. For these reasons, a generator model like that of Equation (2.21) which neglects the dynamics of the interconnected electrical system is sufficient.

$$\frac{dW}{dt} = \frac{1}{J}(M - M_e - W \cdot R) \qquad (2.21)$$

M is the turbine torque, M_e is an opposing torque acting on the machine rotor, as a result of the electrical power being produced, and R is the generator rotational losses caused by windage, bearing friction and field excitation. The rotational losses are assumed to be proportional to the turbine shaft speed. W is the rotational speed of the generator shaft, and J is the inertia of the system.

Assuming that the opposing electrical torque is constant, Equation (2.21) may be rewritten in small signal per unit form, for changes about a steady state operating point.

$$\frac{w(s)}{m(s)} = \frac{1}{\tau_m \cdot s + r} \tag{2.22}$$

$$\tau_m = \frac{W_0 \cdot J}{M_0}$$

$$r = \frac{W_0 \cdot R}{M_0}$$

The transformation from the time domain to the Laplace domain has been performed assuming zero initial conditions. Further simplification is possible in most practical applications because the effects of rotational losses have little effect on shaft speed, due to the enormous amount inertia contained in the system, so it is customary to assume $r \approx 0$ [2,4,9].

2.6 System Transfer Function

The penstock water model given by Equation (2.10) may be combined with the turbine equations of (2.14) and (2.15) to formulate a system the transfer function. The development begins by using Equation (2.10) to eliminate q_t in Equation (2.14), making note that the turbine constant $a_{12} = 0$.

$$\frac{-h_t(s)}{(\tau_w s + k)} = a_{11} h_t(s) + a_{13} g_t(s)$$

$$h_t(s) = \frac{-a_{13}(\tau_w s + k)}{1 + a_{11}(\tau_w s + k)} \cdot g_t(s) \tag{2.23}$$

Now, the above equation may be substituted into (2.15) to find an expression for turbine torque.

$$m(s) = \frac{-a_{21} a_{13}(\tau_w s + k)}{1 + a_{11}(\tau_w s + k)} \cdot g_t(s) + a_{22} w(s) + a_{23} g_t(s)$$

$$m(s) = \frac{a_{23} + (a_{23} a_{11} - a_{21} a_{13})(\tau_w s + k)}{1 + a_{11}(\tau_w s + k)} \cdot g_t(s) + a_{22} w(s)$$

The expression above for turbine torque above may be combine with the torque–speed transfer function of Equation (2.22) to find a single relationship for generator speed as a function of wicket gate position.

$$w(s) = \frac{1}{(\tau_m s + r)} \cdot \left\{ \frac{a_{23} + (a_{23}a_{11} - a_{21}a_{13})(\tau_w s + k)}{1 + a_{11}(\tau_w s + k)} \cdot g_t(s) + a_{22} w(s) \right\}$$

$$w(s) = \frac{a_{23} + (a_{23}a_{11} - a_{21}a_{13})(\tau_w s + k)}{(\tau_m s + r - a_{22})(1 + a_{11}(\tau_w s + k))} \cdot g_t(s)$$

Finally, the gate actuator dynamics may be augmented to form a transfer function relating gate control input to generator speed using Equation (2.20).

$$w(s) = \frac{a_{23} + (a_{23}a_{11} - a_{21}a_{13})(\tau_w s + k)}{(\tau_m s + r - a_{22}) \cdot (1 + a_{11}(\tau_w s + k)) \cdot \tau_g s} \cdot u_c(s) \qquad (2.24)$$

Equation (2.24) may be further simplified to Equation (2.25) if the rotational losses are considered negligible, and the penstock butterfly valve is in the fully open position, so that water losses are also negligible.

$$w(s) = \frac{a_{23} + (a_{23}a_{11} - a_{21}a_{13}) \cdot \tau_w s}{(\tau_m s - a_{22}) \cdot (1 + a_{11}\tau_w s) \cdot \tau_g s} \cdot u_c(s) \qquad (2.25)$$

2.7 Turbine Characteristics

As stated previously, the behavior of the Kakabeka units in an online mode of operation is the same as other hydro turbines; incremental increases in gate opening create a proportionate amount a shaft torque. Under normal operating conditions the large interconnected power system maintains the unit speed so that increases in shaft torque result in a net increase in power output. The only adverse effect that the gate leakage has is a measurable but small positive power output when the wicket gates are fully closed. Only in an abnormal islanding condition, where the Kakabeka units may be left connected to a small isolated load, would the wicket gate leakage cause a possible speed-governing problem. Thus it is sufficient to use standard speed governing techniques on the units while online, with the provision that over-speed detection and tripping is present.

It is the off-line mode of operation that requires further investigation, since speed governing is impossible without the added use of the butterfly valve. To determine the best means of providing speed control with the wicket gates and the butterfly valve, one must investigate the steady-state relationship between unit speed, butterfly valve position, and wicket gate position. Simple fluid flow relationships may be used for the butterfly valve, wicket gates, and the turbine. In the following analysis, the turbine characteristics will be assumed ideal over the full operating range and the bypass valve neglected. Also, the assumption that the water is incompressible and the penstock inelastic will be used so

that Euler's equation for fluid flow in a conduit may be applied to account for the penstock behavior.

Under steady state conditions the differential elements with respect to time in Equations (2.10) and (2.21) may be set to zero so that:

$$H = H_t + H_b \tag{2.26}$$

$$M = W \cdot R \tag{2.27}$$

To derive Equation (2.26), the variables of (2.10) expressed as per-unit deviations from a steady-state operating point have been substituted with engineering units, and the butterfly valve head loss assumed proportional to $kq(t)$ has been replaced with the actual head loss H_b, expressed in meters of water. In Equation (2.21) the opposing electrical torque acting on the rotor has been taken as $M_e=0$, since we are considering the off-line mode of operation only.

Equation (2.26) may be substituted into (2.12) and then combined with Equation (2.17) to express the turbine head as a function of gate/valve position and total available head:

$$H_t = \frac{(C_b g_b)^2}{(C_t g_t)^2 + (C_b g_b)^2} \cdot H \tag{2.28}$$

This may be combined again with Equation (2.17) to express turbine flow in the same variable set.

$$Q = \left\{ \frac{(C_t g_t)^2 \cdot (C_b g_b)^2}{(C_t g_t)^2 + (C_b g_b)^2} \cdot H \right\}^{1/2} \tag{2.29}$$

Equation (2.27) may be combined with Equation (2.16) to form a relationship for generator speed.

$$W = \left\{ \frac{\gamma \rho g}{R} \cdot H_t \cdot Q \right\}^{1/2} \tag{2.30}$$

Now, Equation (2.28), (2.29) and (2.30) may be combined together as follows:

$$W = \left\{ \frac{\gamma \rho g}{R} \right\}^{1/2} \cdot \left\{ \frac{c^3 x H^3}{(c+x)^3} \right\}^{1/4} \tag{2.31}$$

$$c = (C_b g_b)^2$$

$$x = (C_t g_t)^2$$

Although it is not entirely obvious, W in Equation (2.30) and (2.31) exhibits a maximum for a given wicket gate and butterfly valve position. If the turbine is to be controlled by fixing the butterfly valve at a partial opening, and the wicket gates are used to regulate speed, then the maximum speed achievable may be determined by differentiating W with respect to x.

$$\frac{dW}{dx} = \left\{\frac{\gamma\rho g}{R}\right\}^{1/2} \cdot \left\{\frac{1}{4} \cdot \frac{(cH)^{3/4} \cdot (c-2x)}{x^{3/4} \cdot (c+x)^{7/4}}\right\}$$

The maximum turbine speed is achieved when $x=½.c$ or in more practical terms, when the turbine head is twice that of the butterfly valve head loss ($H_t=2H_b$). In terms of gate position, the maximum speed occurs at:

$$g_t = \frac{C_b g_b}{\sqrt{2}C_t} \qquad (2.32)$$

Proof that this point is indeed a maximum and not a minimum, may be shown with the second derivative of W with respect to x.

$$\frac{d^2w}{dx^2} = \left\{\frac{\gamma\rho g}{R}\right\}^{1/2} \cdot \left\{\frac{3}{16} \cdot \frac{(cH)^{3/4}(4x^2 - 4xc - c^2)}{x^{7/4}(c+x)^{11/4}}\right\}\Bigg|_{x=½c} < 0$$

The second derivative is less then zero at $x=½c$ indicating that the point is a maximum.

Figure 2-2 shows the measured and theoretical steady-state turbine speed curves of the Kakabeka G1 unit. Note that the turbine exhibits a peak operating speed for a given set of wicket gate and butterfly valve openings: Similar results were obtained for the other turbines. Since no means of measuring penstock flow or turbine torque was available at the plant, the experiment data shown in Figure 2-2, and that collected from the other units, was used to compute the various unit constants as described below. These constants are summarized in Table 2-1.

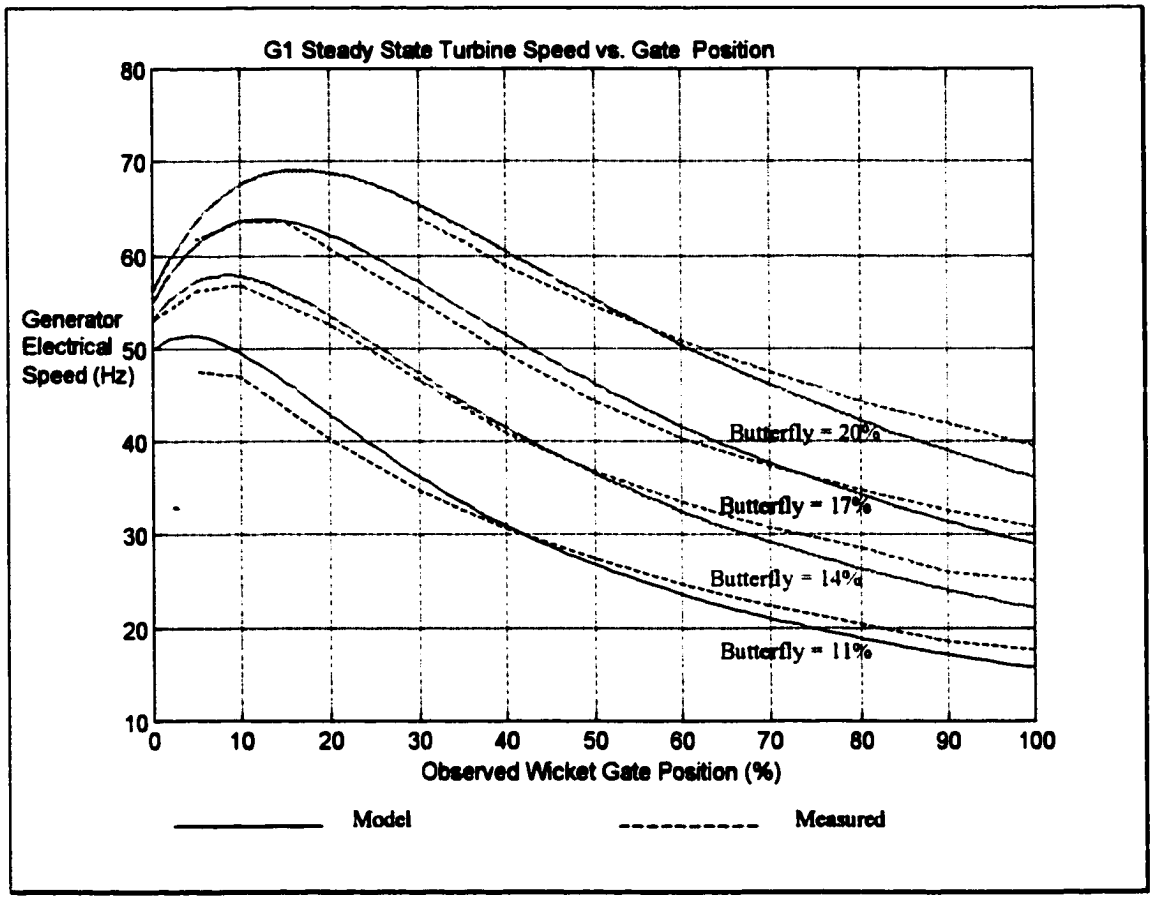

Figure 2-2 Steady State Turbine Characteristics

The full load penstock flow Q, the turbine power in megawatts, and efficiency γ, given in Table 2-1 were taken from reference [17]. The turbine flow constant C_t was computed using Equation (2.17) assuming full load flow, a normal operating head, and a fully open butterfly valve. The butterfly valve coefficients were computed from Equation (2.32) based upon the peak operating points observed in the experimental data. As well, the rotational loss factor R was extracted from the operating data at the observed peak using Equation (2.30). The inertia J was determined experimentally by observing the time required for the turbine to reach 36.8% of rated speed following a unit shutdown. The measured time was taken to be J/R as per Equation (2.21). The wicket gate leakage was estimated at 10% for all turbines based upon the residual power observed while the generator was connected to the power grid and the wicket gates were fully closed.

Discrepancies between the curves obtained experimentally and those defined by Equation (2.31) are thought to be attributed mostly to non-ideal turbine behavior, and small inaccuracies in the computed constants. The throttling action of the butterfly valve can significantly reduce the effective turbine head and disrupt the water flow patterns at the turbine inlet; both of which impact efficiency of the conversion from waterpower to mechanical power, and make the turbine behave in a non-ideal manner.

Table 2-1 Generating Unit Constants

Net Water Head = 54.0 m (Surge Tank Elevation – Tail Race Elevation)

Generator	Full Load Flow (m^3/s)	Full Load Power (Mw)	Turbine Efficiency	Turbine Flow Constant - Ct (m^(5/2)/s)	Butterfly Constant - Cb (m^(5/2)/s)	Inertia - J (Kg*m^2)	Rotational Losses - R (Kg*m^2/s)
G1	11.03	5.12	0.88	1.50	2.65	94249	628.3
G2	10.52	5.12	0.92	1.43	2.53	94249	628.3
G3	11.03	5.12	0.88	1.50	2.65	94249	628.3
G4	17.10	8.19	0.90	2.33	5.38	227736	1167.9

2.8 Operating Point Selection

Determining an on-line operating point is straightforward since consideration need not be given to the effects of wicket gate leakage. In the off-line mode, the steady state operating point is selected based upon the desired operating speed of 60Hz. It is evident from Figure 2.2 that two valid steady-state operating points will exist on the speed curves that intersect the 60Hz grid line. Curves falling short of this value hold no valid operating points. Likewise curves formed by larger butterfly valve opening will also not contain valid operating points. The wicket gate opening at the point of intersection for the theoretical curves may be determined by solving the following 3rd order polynomial derived from Equation (2.31):

$$(c+x)^3 - \left(\frac{\gamma\rho g}{W^2 R}\right)^2 \cdot c^3 H^3 \cdot x = 0 \qquad (2.33)$$

Given the rated turbine speed W_* specified in rad/sec of shaft speed, and the desired butterfly valve opening such that $c = (C_b g_{b*})^2$, the steady state wicket gate opening g_{t*} may be found by solving for x in Equation (2.33). From these three values, one may compute all the other pertinent steady-state operating parameters.

With the on-line and off-line operating points known, all of transfer function parameters contained in Equation (2.24) may be computed. Table 2-2 summarizes the steady state operating points and the transfer function parameters for the four Kakabeka generating units. For these values, the full load operating point of each turbine has been selected as both the per-unit base, and the on-line operating point.

Table 2-2 Model Parameters for Steady State Operating Points

Unit Operating Mode	Turbine Speed (Hz) w_r	Butterfly Valve Position g_{BV}	Wicket Gate Position g_r	Observed Gate Position g'_r	Turbine Head (m) H_r	Turbine Flow (m^3/s) Q_r	Turbine Torque (N*m) M_r	Turbine Constants a_{11}	a_{12}	a_{13}	a_{21}	a_{22}	a_{23}	Water Starting Time (s) Tw	Butterfly Head Loss (s/m^2) K	Mech. Time Const. (s) Tm	Rotation Loss (Kgm^2/s) r	Gate Time Const. (s) Tg'
G1-G3 Off-Line	60	20%	12.2%	2.5%	48.22	1.28	18229	0.065	0.000	0.945	0.173	-0.103	0.844	1.287	1.851	15.49	0.103	7.22
	60	20%	46.4%	40.4%	19.84	3.10	18231	0.383	0.000	0.606	0.422	-0.103	0.223	1.287	4.500	15.49	0.103	7.22
G1-G3 On-Line	60	100%	100.0%	100.0%	54.00	11.03	176488	0.500	0.000	1.000	1.500	-1.000	1.000	1.287	0.000	15.49	0.103	7.22
G4 Off-Line	60	16%	12.0%	2.2%	48.86	1.95	30458	0.063	0.000	0.951	0.171	-0.103	0.861	0.995	1.669	20.14	0.103	16.67
	60	16%	51.0%	45.5%	18.63	5.12	30455	0.434	0.000	0.587	0.449	-0.103	0.203	0.995	4.376	20.14	0.103	16.67
G4 On-Line	60	100%	100.0%	100.0%	54.00	17.10	294932	0.500	0.000	1.000	1.500	-1.000	1.000	0.995	0.000	20.14	0.103	16.67

Each of the turbines has two distinctive off-line operating points (see Figure 2-2). The first operating point has a characteristic typical of hydro turbines; increased wicket gate opening provides increased flow, positive torque, and increased speed. The second operating point is very distinctive from typical hydro turbine operation; increased wicket gate opening does produce increased flow, however this flow also results in significant head loss at the butterfly valve and diminished water power at the turbine. The loss in turbine head is more significant than the increased flow, thus resulting in lower shaft torque and reduced speed.

Though unusual this "inverse characteristic" has some significant advantages over the other operating point. First, relationship between gate position and turbine speed is quite linear and the operating range of the wicket gates and resultant speed is large. This is important since fluctuations in surge tank water levels or small errors in butterfly valve positioning may adversely effect any efforts made to regulate speed. With the expanded operating range of the inverse characteristic, any speed governing strategy utilized will be better able to tolerate such deviations.

Secondly, the wicket gates never need to operate within the bottom range of wicket gate movement, thus eliminating any ill effects that might be caused by the bypass valve. Experimental attempts to speed govern turbines 1-3 on the more traditional "forward characteristic" was hampered by movements in the bypass valve. This also explains why the plant operators used to find the task of manually synchronizing the Kakabeka units tedious and time consuming; they were always operating in the normal turbine characteristic region rather than the inverse characteristic region. Prior to the findings of this thesis, the inverse mode of operation was never revealed or utilized for speed control, and the bypass valves would adversely affect manual control efforts.

From the arguments above it is clear that the inverse turbine characteristic must be chosen to provide speed regulation in an off-line mode of operation. It will be necessary for an automatic speed governor to first position the butterfly valve at the appropriate fixed partial opening, and then use wicket gates within the inverse operating range of the turbine to attempt to regulate unit speed for generator startup & synchronization. Once the unit is successfully connected to the power system, the speed governor must fully open the butterfly valve to extract the maximum possible power from the turbine. At this point the wicket gates will again operate in a manner typical of hydro turbines, and may be adjusted so as to maintain frequency and power output at a desired level. This behavior is captured it the transfer function of (2.24); The steady state gain of the transfer function for the on-line parameters given in Table 2-2 is positive, while the off-line parameters result in a negative steady state gain.

2.9 Summary

The linear model formed by Equation (2.24) and the parameters for Table 2-2 describes the dynamics of Kakabeka generating units, and may be used to proceed with governor design.

Each turbine exhibits two distinctive modes of operation with differing dynamics: The first is termed the "on-line" mode and occurs when the generating unit is connected to the power system. The second "off-line" mode occurs when the generator is disconnected from the power system.

In the on-line mode, turbine behavior is normal and standard speed governing techniques may be applied. In the off-line mode, severe wicket gate leakage requires that both the wicket gates and a penstock butterfly valve be used to provide adequate speed governing. The turbine characteristics are the opposite of what one might expect: Under steady state conditions, increased gate opening causes generator frequency to fall not rise. Special consideration will have to be given to governor design due to the characteristics exhibited by the turbines in the off-line mode

Chapter 3

Speed Droop Governing

3.1 Introduction

In this chapter a digital speed droop governor scheme is considered for control of the Kakabeka Generators. A gain scheduling arrangement is employed to account for the differing dynamic characteristics resulting from the on-line and off-line operating modes. For each mode of operation, the stability boundaries of the governor parameters are investigated, and an output feedback algorithm is used to assist in finding the unknown controller gains. An outline of the software used to implement the governor on an industrial programmable controller is presented, and the experimental performance of the turbines is compared to the theoretically developed model of Chapter 2.

3.2 Speed Droop Governing

Speed droop governor systems are common to low and medium head hydro generating stations. Nearly all of Ontario Power Generation's hydroelectric facilities in Northwest Ontario utilize a droop governor scheme of one form or another. And since the operating and maintenance staff of these facilities are familiar with its operation, this scheme becomes a logical choice for the Kakabeka Plant.

Figure 3-1 shows a block diagram for a speed droop governor. The wicket gates are forced open or closed based upon error Δw between the desired speed w_0 and measured speed w. The external input signal δ is normally provided for gate control or frequency adjustment under steady state conditions.

The droop compensation consists of two parallel control branches, each providing feedback from the wicket gate position to the wicket gate actuator. The first branch uses a proportional gain R_p commonly referred to as the permanent droop setting. The second branch consists of a frequency limited derivative element. The parameter R_t is known as the transient droop setting, and τ_r is referred to as the reset time.

The permanent droop determines the amount of gate opening (or closing) that will result with a fixed frequency error of Δw, under steady state conditions. The permanent droop is normally specified as the percent of rated frequency required to drive the wicket gates to the fully open position. Because permanent droop controls the amount of prime mover energy added or removed from an interconnected transmission system, its value is usually specified based on system stability considerations and not on machine characteristics. Ontario Power Generation requires that a permanent droop setting of 4% be used on all hydro turbines in Northwest Ontario [16].

The transient droop and reset time together essentially provide derivative feedback on the gate position under transient conditions. It is the transient droop characteristic that is set to maintain governor stability, and it does this by providing improved gain and phase margins around gain crossover frequency.

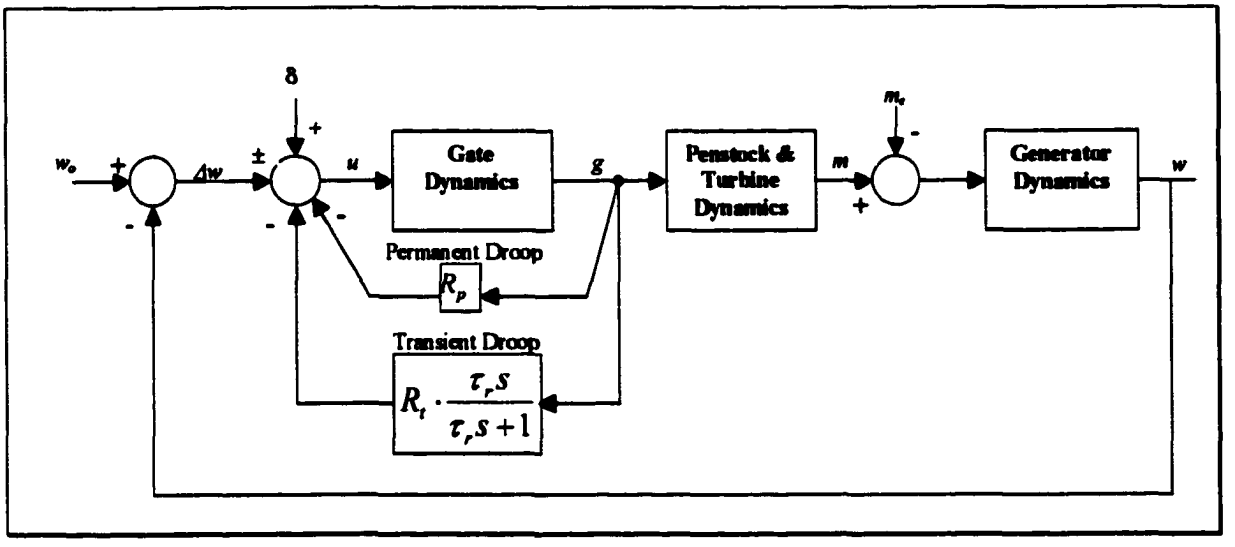

Figure 3-1 Speed Droop Governor Control

In consideration of speed governing for Kakabeka, two points are worth noting; First the error signal Δw will be taken as frequency error between the power system and the generator measured directly in Hz. This essentially provides an additional gain on the gate actuator signal and improves overall governor performance [4]. This extra gain may be accounted for in the model of Chapter 2 by multiplying Equation (2.20) by a factor of 60. In general, [4] makes note of the fact that an overall gain of 5-10 in the gate actuator dynamics is desirable. Secondly, the typical assignment of a (+) polarity on the frequency error signal has been replaced with a sign change (±) to signify that a polarity reversal will be necessary to account for the inverse turbine characteristics while operating in the off-line mode.

The effects of permanent and transient droop may be studied further by investigating the open loop frequency response of the governor system shown in Figure 3-1. The penstock, turbine, and generator dynamics may been taken as:

$$H(s) = \frac{w(s)}{g_t(s)} = \frac{a_{23} + (a_{23}a_{11} - a_{21}a_{13}) \cdot \tau_w s}{(\tau_m s - a_{22}) \cdot (1 + a_{11}\tau_w s)}$$

based upon Equation (2.24) and the values in Table 2-2.

The gate actuator dynamics including gain compensation for direct frequency feedback is:

$$G(s) = \frac{g_t(s)}{u_c(s)} = \frac{60}{\tau_g s}$$

And the permanent and transient droop compensation denoted as *D(s)*, may be shown as part of the forward loop characteristic by:

$$K(s) = \frac{1}{1 + G(s)D(s)}$$

so that the closed loop system in Figure 3-1 may be represented as unity feedback around the open loop transfer function *K(s)G(s)H(s)*.

For permanent droop compensation alone,

$$K(s) = \frac{\tau_g s}{\tau_g s + 60 \cdot R_p}$$

and for transient droop alone,

$$K(s) = \frac{\tau_g \tau_r s + \tau_g}{\tau_g \tau_r s + (\tau_g + \tau_r 60 R_t)}$$

Figures 3-2 and 3-3 provide Bode plots of the on-line and off-line transfer function models derived in Chapter 2. In each Figure the independent effects of permanent and transient droop *K(s)*, have been plotted along side the open loop dynamics $\pm G(s)H(s)$. In both cases the reset time τ_r has been taken as $5\tau_w$, so that the transient droop provides phase and gain compensation around the gain crossover frequency. The sign applied to the open loop system is dependent upon the operating mode.

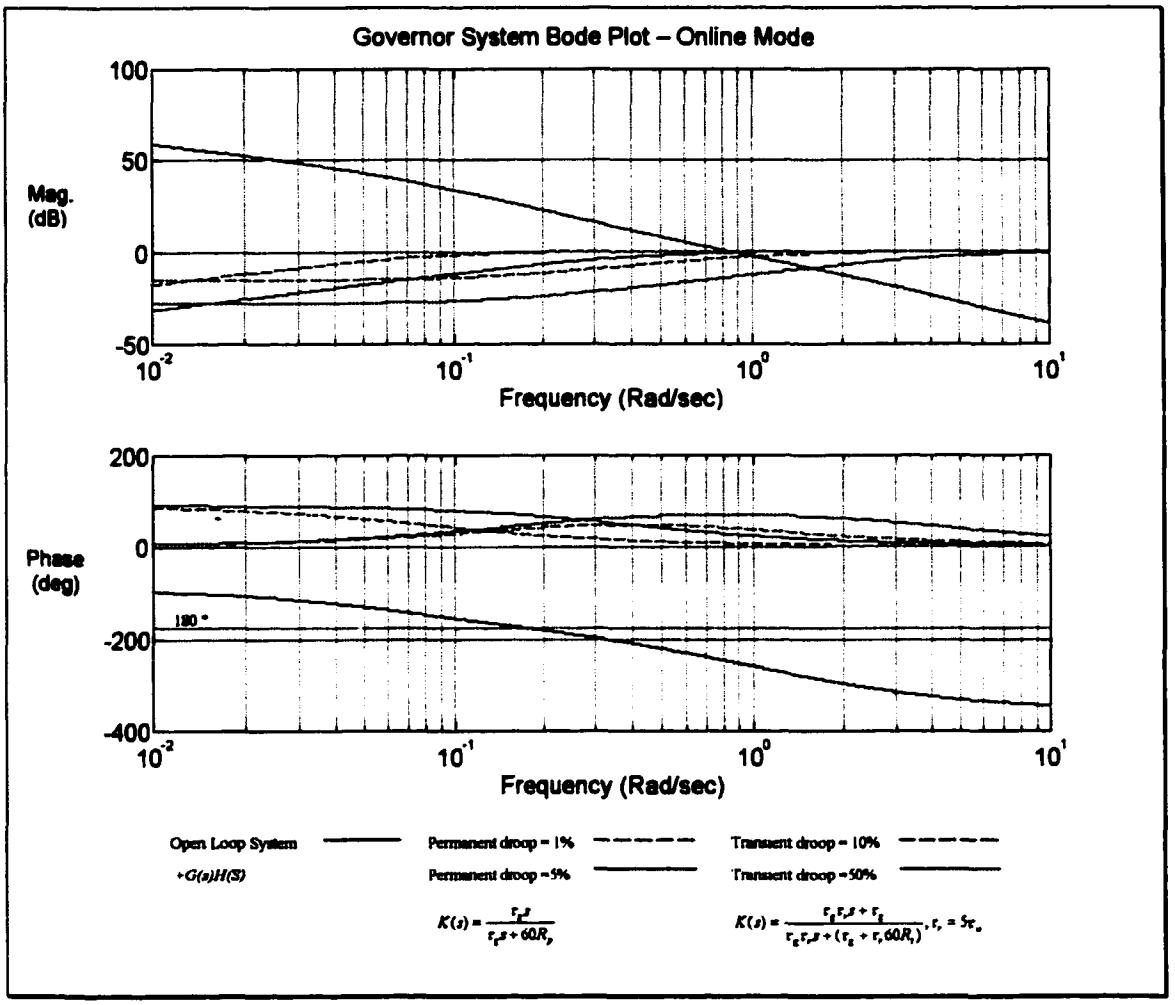

Figure 3-2 Governor system Bode Plot - Online Mode

From Figure 3-2 one can see that open loop system without compensation is unstable. This is due to the in part to the phase shift caused by the gate and generator dynamics, but also because of the water hammer effect in the penstock. Under transient conditions, an incremental gate opening causes the turbine water pressure and speed to decrease for a short period of time, until the mass flow of water in the penstock can accelerate to a new steady-state value. Thus, the effects of water hammer also create phase lag in the open loop system, and reduce stability.

The permanent droop limits steady-state open loop gain by canceling the integrator in the gate dynamics, and the transient droop provides a positive phase shift at the crossover frequency. Since low values of permanent droop are typically required to obtain tight frequency regulation of the interconnected power system, transient droop compensation must be used to stabilize the closed loop system.

The inverse characteristic exhibited by the turbine in the off-line mode of operation, results in a reduced phase shift of the open loop transfer function, and closed loop

stability without compensation. This is depicted in Figure 3-3. The reduced phase shift is a result the of inverse turbine behavior coupled with the effects of water hammer. An incremental gate opening to slow the generator speed is aided by the transient response of the mass flow of water in the penstock.

Although the system is closed loop stable without any governor compensation, the phase and gain margins are poor and instability may result if unmodeled dynamics are excited. From the Bode plot in Figure 3-3, it appears that permanent droop alone may provide adequate compensation, while further improvements in phase and gain margins are possible with the addition of transient droop.

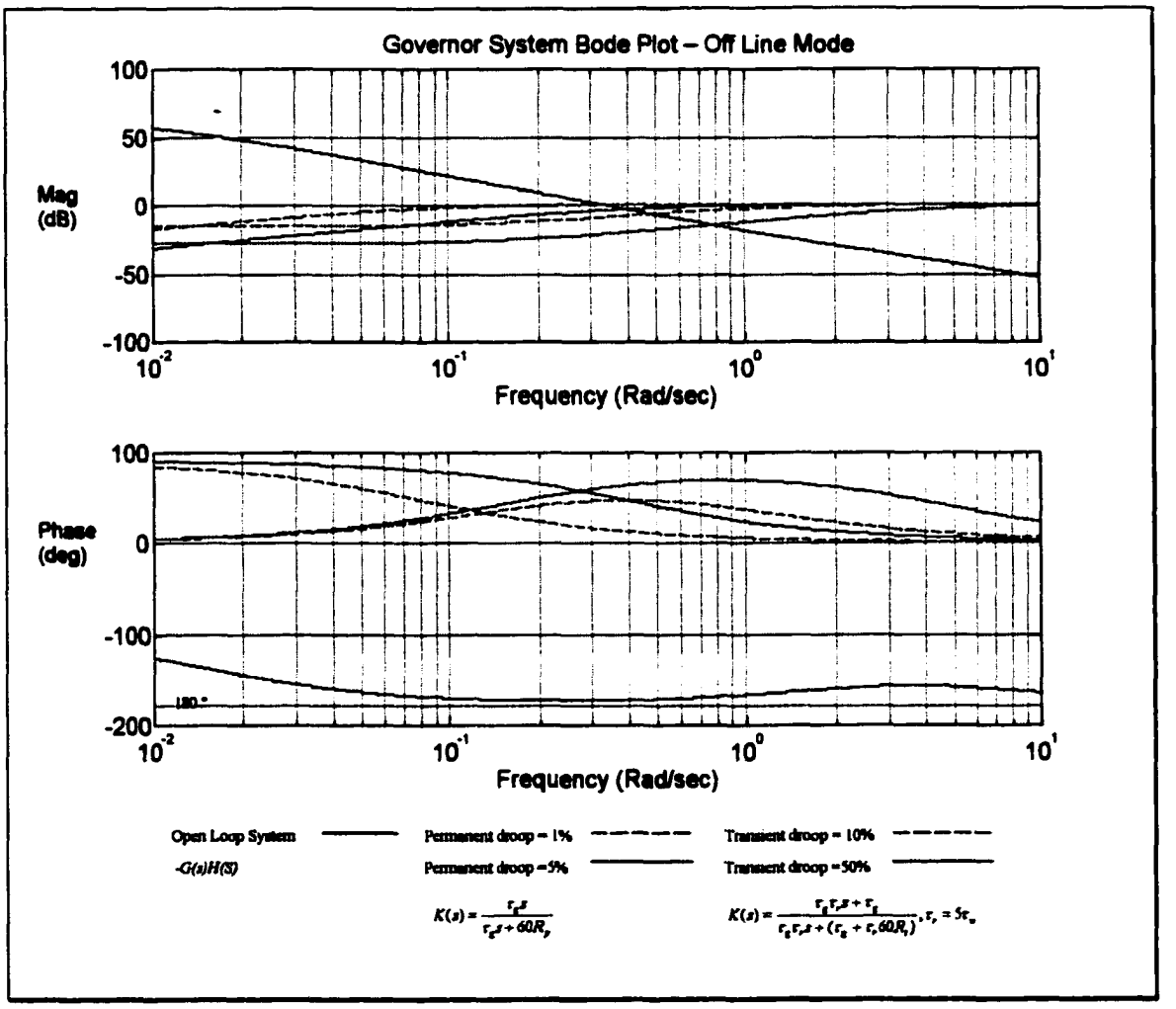

Figure 3-3 Governor System Bode Plot - Off Line Mode

3.3 Stability Region of Governor Settings

In [9] Hovey showed that the stability of the speed droop governor for the turbine and water dynamics of Equation (3.1), and the generator dynamics of Equation (3.2), is dependent on the pole locations of the Laplace domain polynomial given by Equation (3.3).

$$m(s) = \frac{1 - \tau_w s}{1 + \frac{1}{2}\tau_w s} \cdot g(s) \tag{3.1}$$

$$w(s) = \frac{1}{\tau_m s} \cdot (m(s) - m_e(s)) \tag{3.2}$$

$$s^3(\tfrac{1}{2}R_t\tau_m\tau_w\tau_r) + s^2(R_t\tau_m\tau_r - \tau_m\tau_r) + s(\tau_r - \tau_w) + 1 = 0 \tag{3.3}$$

Equation (3.3) is the simplified characteristic polynomial of the transfer function relating electrical torque disturbance input m_e to the generator speed output, taken from the block diagram shown in Figure 3-1. The governor will be stable to step changes in m_e if all the poles of (3.3) lie in the left half plane.

By way of a simple Routh-Hurwitz test, Hovey showed that a closed stability region existed for the droop governor based on two parameters λ_1 and λ_2 [9]. The stability region is given as:

$$\lambda_1 = \frac{1 - 1.5\lambda_2}{1 - \lambda_2} \tag{3.4}$$

With λ_1 and λ_2 being functions of the water starting time τ_w, mechanical time constant τ_m, transient droop R_t and reset time τ_r.

$$\lambda_1 = \frac{\tau_w}{R_t\tau_m}$$

$$\lambda_2 = \frac{\tau_w}{\tau_r}$$

By searching out an aesthetically pleasing time response within the region of stability, Hovey was able to develop the following tuning procedure[9]:

$$R_t = \frac{2\tau_w}{\tau_m},\ \tau_r = 4\tau_w \tag{3.5}$$

This is an important result and one that is particularly useful for governor system tuning.

To assess the stability region for the two operating modes defined in Chapter 2, Hovey's work may be repeated in a more generalized framework. To account for the changes in the turbine and water model, the transfer function of Equation (3.1) may be restated with coefficient elements n_1, n_2 and d_1.

$$m(s) = \frac{n_1 - n_2 \tau_w s}{1 + d_1 \tau_w s} \cdot g(s) \qquad (3.6)$$

The sign reversal that occurs in the governor control loop between the on-line and off-line modes, can be accounted for by modifying the polynomial equation of (3.3) as:

$$s^3(d_1 R_t \tau_m \tau_w \tau_r) + s^2(R_t \tau_m \tau_r \mp n_2 \tau_w \tau_r) \pm s(n_1 \tau_r - n_2 \tau_w) \pm n_1 = 0 \qquad (3.7)$$

Using a Routh-Hurwitz Table [18], one may determine the conditions (if any) under which all of the poles of Equation (3.7) are in the left half plane:

s^3	$(d_1 R_t \tau_m \tau_w \tau_r)$	$\pm(n_1 \tau_r - n_2 \tau_w)$
s^2	$(R_t \tau_m \tau_r \mp n_2 \tau_w \tau_r)$	$\pm n_1$
s^1	$\dfrac{\pm(R_t \tau_m \tau_r \mp n_2 \tau_w \tau_r)(n_1 \tau_r - n_2 \tau_w) \mp (n_1 d_1 R_t \tau_m \tau_w \tau_r)}{(R_t \tau_m \tau_r \mp n_2 \tau_w \tau_r)}$	0
s^0	$\pm n_1$	0

For the on-line mode of operation, assuming small deviations in speed so that $a_{22}=0$, the turbine and water model may be taken as:

$$m(s) = \frac{a_{23} + (a_{23} a_{11} - a_{21} a_{13}) \tau_w s}{(1 + a_{11} \tau_w s)} \cdot g(s)$$

Comparing this to Equation (3.6) and substituting the turbine parameters from Table 2-2, the coefficients n_1, n_2 and d_1 evaluate to:

$$n_1 = a_{23} \approx 1.0$$
$$n_2 = (a_{21} a_{13} - a_{23} a_{11}) \approx 1.0$$
$$d_1 = a_{11} \approx 0.5$$

Equation (3.7) will be stable with all poles in the left half plane if the elements on the right of the Routh-Hurwitz table have the same sign (+ in this case). The polynomial of Equation (3.7) is stable if the following conditions are met:

1. $d_1 R_t > 0$
2. $R_t \dfrac{\tau_m}{\tau_w} > n_2$

3. $R_t \frac{\tau_m}{\tau_w} > \frac{n_2(n_2 - n_1 \tau_r/\tau_w)}{n_2 + n_1(d_1 - \tau_r/\tau_w)}$ (3.8)

4. $n_1 > 0$

Of the 4 conditions, 3 is the most restrictive and is equivalent to that derived in [9]. Condition 1 requires only that R_t is positive. Condition 2 is less restrictive than Condition 3 given the turbine constants, and the values of τ_r/τ_w that are of interest. The turbine model alone satisfies condition 4. The relationship defined by Equation (3.8) is shown graphically in Figure 3-4.

For the off-line mode, with the head losses due to the butterfly valve taken into account, and assuming small deviations in speed so that $a_{22}=0$, the turbine and water model may be taken as:

$$m(s) = \frac{a_{23} + (a_{23}a_{11} - a_{21}a_{13})(\tau_w s + k)}{(1 + a_{11}(\tau_w s + k))} \cdot g(s) \quad (3.9)$$

Again, comparing this to Equation (3.6) and substituting the turbine parameters from Table 2-2, the coefficients n_1, n_2 and d_1 evaluate to:

$$n_1 = \frac{a_{23} + (a_{23}a_{11} - a_{21}a_{13})k}{(1 + a_{11}k)} \approx -0.2$$

$$n_2 = \frac{(a_{21}a_{13} - a_{23}a_{11})}{(1 + a_{11}k)} \approx 0.063$$

$$d_1 = \frac{a_{11}}{(1 + a_{11}k)} \approx 0.141$$

Based on the Routh-Hurwitz table from above, the conditions for stability for the off-line mode of operation are:

1. $d_1 R_t > 0$ (3.10)

2. $R_t \frac{\tau_m}{\tau_w} > -n_2$

3. $R_t \frac{\tau_m}{\tau_w} > \frac{n_2(n_2 - n_1 \tau_r/\tau_w)}{-n_2 + n_1(d_1 + \tau_r/\tau_w)}$

4. $n_1 < 0$

Condition 1 requires that R_t be positive. Condition 2 and Condition 3 are less restrictive since they require that R_t be approximately greater than $-n_2$. And condition 4 is satisfied by the turbine parameters alone. Thus Equation (3.10) becomes the necessary condition for stability.

It is interesting to note that without the sign change in the governor loop for the off-line mode no stability region exists. The Routh-Hurwitz test confirms the need to change the control structure based upon the inverse characteristic of the turbine in the off-line operating mode.

Figure 3-4 shows graphically the stability regions for each of the operating modes. Note that Hovey's governor tuning rule falls within a common stability region, allowing the same values of transient droop and reset time to be used for both operating modes. Also, the computed stability regions agree closely with the Bode plots presented in the previous section.

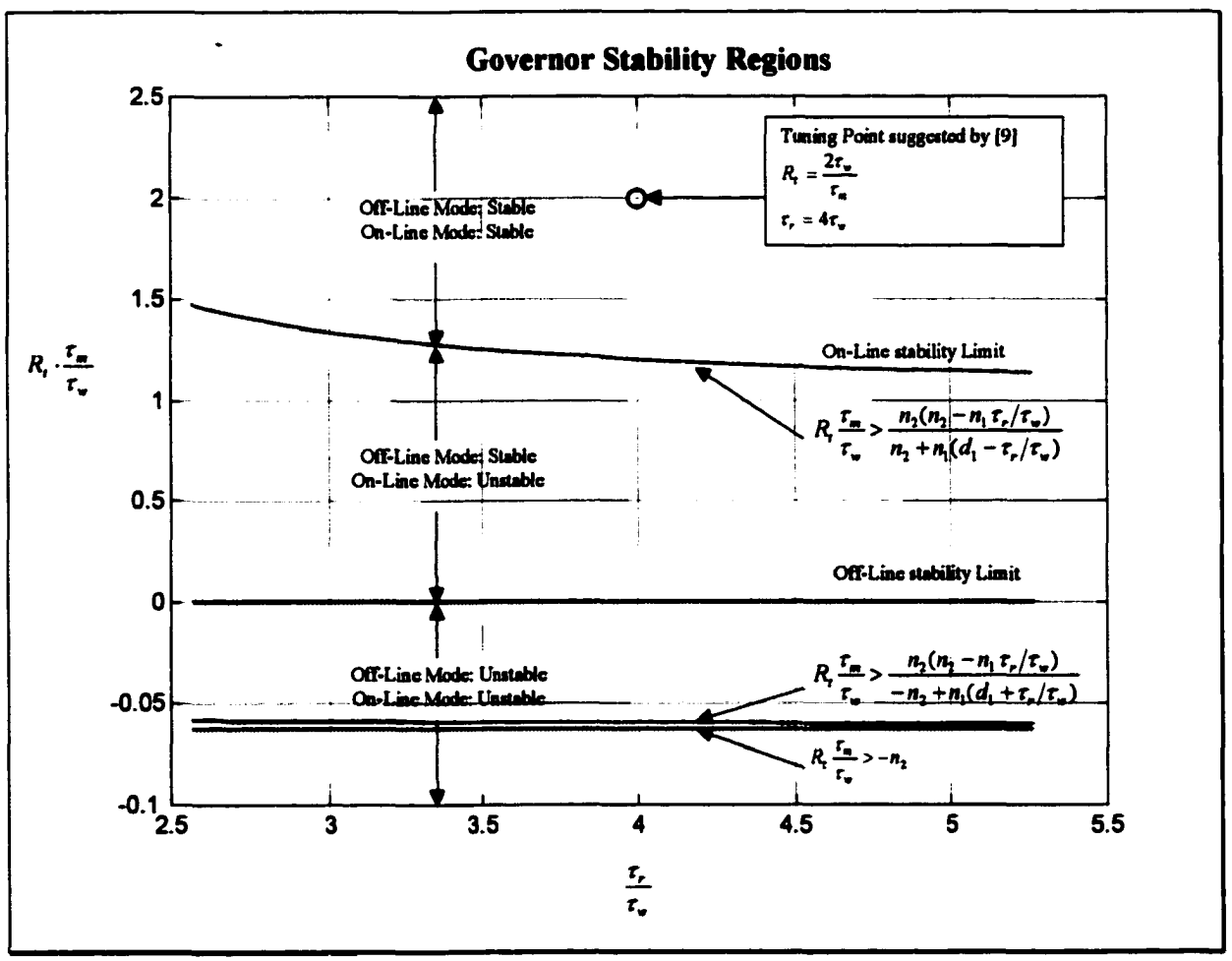

Figure 3-4 Governor Stability Regions

In the development above and in that of [9] a number of assumptions have been made to derive the polynomials of Equations (3.3) and (3.6). First the permanent droop setting has been assumed negligible under transient conditions, The changes in per unit speed are assumed to be small so that the effects of the turbine constant a_{22} may be neglected. The

rotational losses or "load self regulation factor" is assumed to be negligible, and the gate actuator time constant is neglected.

A number of authors have expanded upon Hovey's work by narrowing the number of assumptions and redefining the stability region shown above. Modified tuning rules are summarized in [4] while good treatment of the modified stability regions is given in [10]. In [10] consideration is given to both permanent droop and rotational losses. In both cases the stability boundaries first defined by Hovey are expanded providing an extra degree of robustness when considering the tuning rules of Equation (3.5).

3.4 Digital Speed Droop Governor

Figure 3-5 is a block diagram of the digital governor control system implemented at Kakabeka GS. The governor logic consists of 3 components: A speed droop governor block, a frequency tracking control block and a wicket gate setpoint control block.

The droop governor block shown at the bottom of the figure is the discrete time equivalent of that present in Figure 3-1. It consists of permanent and transient droop feedback elements. The discrete transient droop component has been derived from its continuous time counterpart by suitable Z-domain transformation with a zero order hold element [15].

$$Z\left\{R_t \cdot \frac{\tau_r s}{\tau_r s+1} \cdot \frac{1-e^{-Ts}}{s}\right\} = R_t \cdot \frac{(z-1)}{(z-e^{-T/\tau_r})} \qquad (3.11)$$

The frequency-tracking block is a discrete proportional + integral (PI control) element enabled whenever the generator is operating in an off-line mode. With w_{sp} set to the power system frequency, this control element nulls any frequency error between the power system and the generator under steady state conditions. The discrete integrator mimics that of a continuous time integrator by way of a trapezoidal summing rule. The present integral of error i_0 is the sum of the past integral of error i_1, and the area sum of the control error e_0, e_1 over the last sampling period T assuming linear interpolation between adjacent error samples.

$$i_0 = i_1 + \frac{T}{2}(e_0 + e_1)$$

This may be written as the Z-domain transfer function:

$$\frac{I(z)}{E(z)} = \frac{T}{2} \cdot \frac{z+1}{z-1} \qquad (3.12)$$

The speed matching between the generator and the system is required to provide generator synchronization to the power system. Although this scheme does not guarantee that the electrical phase angle between the power system and the generator will be zero, small hydraulic disturbances in the system normally produce enough phase crossings to facilitate synchronizing. Otherwise, the external governor input δ may be used disturb the generator speed a small amount to reduce or advance any phase disparity after speed matching is achieved.

The gate setpoint control block functions during the online mode of operation, and provides a means of regulating generated power through wicket gate positioning. Like the frequency-tracking block, this block also has a discrete PI structure and uses the same transfer function.
Under normal power system conditions, the block is enabled and provides wicket setpoint control functionality to a plant operator. However, during power system disturbances when there is error between the desired frequency $w_{sp} = 60\ Hz$ and the actual system frequency w, the block is disabled so that the speed droop governor may react to the frequency error. Disabling this PI loop insures that the gate control will not fight the actions of the speed governing, and that the generator will react in a manner that helps to sustain power system stability.

Ramp limiters are used on both the Frequency setpoint signal and the gate setpoint signal. For the frequency setpoint, the limiter prevents gate actuator saturation during generator startup, while the gate setpoint limiter reduces the effective rate at which the gates move when a setpoint change takes place. This allows the changes in water consumption by the turbine to occur slowly and in a linear fashion so that a plant operator can respond to surge tank water requirements.

The governor control is coordinated with the operation of the butterfly valve and the generator breaker, with programmable logic controller. On generator startup the butterfly valve is opened to the throttled position $gb \approx 20\%$, prior to the governor block being enabled in the off-line operating mode. When the generator achieves synchronization with the power system and the breaker closes, the governor algorithm automatically switches to the online operating mode, and the butterfly valve is forced to the fully open position.

A shutdown sequence is similar: When the plant operator unloads a generator and requests that it is taken off-line, the butterfly valve is first closed to the throttled position. The unit breaker is then tripped and the governor algorithm is switched from the on-line to the off-line mode.

A gain scheduling arrangement is used when the mode of the governor is changed. While off-line the generator dynamics are stabilized by a set of gains applied to the droop governor and the frequency-tracking PI blocks. In the on-line mode, an independent set of gains is applied to the droop and gate setpoint blocks to account for the differing dynamic characteristics.

The governor control algorithm is coded in a basic like language made available by the programming software for the PLC. The algorithm makes use of measured field data collected by way of transducers and an A/D converter. The complete set of algorithm instructions run every scan cycle of the PLC, and upon completion return the gate actuator control signal via a D/A converter. The measurement and conversion of these signals is depicted in Figure 3-5 by the indicated sampling points. Setpoint information enters into the algorithm by way of digital communications from a plant supervisory control and data acquisition system (SCADA).

The governor algorithm accepts a number of inputs defined as:

```
Auto:   BOOL;   (* Governor enable Auto (1) / Man (0)                        *)
Mode:   BOOL;   (* Operating Mode On-Line (1) / Off-Line (0)                 *)
Gsp:    REAL;   (* Gate Setpoint 0.0-100.0 %                                 *)
G:      REAL;   (* Gate Position 0.0 100.0 %                                 *)
Grmp:   BOOL;   (* Gate Setpoint Ramp Limiting Enable (1) / Disable (0)      *)
Grate:  REAL;   (* Gate Ramp Limiting Rate % / sec.                           *)
Fsp:    REAL;   (* Generator Frequency Setpoint Hz                           *)
F:      REAL;   (* Generator Frequency Hz                                    *)
Frmp:   BOOL;   (* Frequency Setpoint Ramp Limiting Enable (1) / Disable (0)*)
Frate:  REAL;   (* Frequency Ramp Limiting Rate Hz/sec                       *)
Umax:   REAL;   (* Maximum Control Signal 0.0 <= Umax <= 1.0                 *)
Umin:   REAL;   (* Minimum Control Signal -1.0<= Umin <= 0.0                 *)
Uman:   REAL;   (* Manual mode Control Signal -1.0 <= Uman <= 1.0            *)
Fm:     Hgov;   (* Off-Line Operating Parameters                             *)
Gm:     Hgov;   (* On-Line Operating Parameters                              *)
```

And the algorithm outputs are:

```
U:      REAL;   (* Control Signal                                  *)
Gset:   BOOL;   (* Gate Ramp Limiting Status On(0)/Off(1)          *)
Fset:   BOOL;   (* Frequency Ramp Limiting Status On(0)/Off(1)     *)
```

Two data structures *Fm* and *Gm* are used to store the off-line and on-line gains for the control algorithm. The format of each structure is the same, and each contains the following elements:

```
Hgov:
        STRUCT
                T:      REAL;           (* Reset Time Constant *)
                Rd:     REAL;           (* Governor Droop Setting *)
                Rt:     REAL;           (* Governor Transient Droop Setting *)
                P:      REAL;           (* Proportional Loop Setting *)
                I:      REAL;           (* Integral Loop Setting *)
                Gmax:   REAL;           (* Maximum Gate Position *)
                Gmin:   REAL;           (* Minimum Gate Position *)
        END_STRUCT;
```

The values of *T*, *Rd* and *Rt* are used for the droop governor control block, while *P* and *I* are used for the gate or frequency tracking control blocks. *Gmax* and *Gmin* allow wicket gate limits to be assigned to each of the operating modes. The elements of the structure are accessed using the language syntax '.' dot operator.

The *Auto* and *Mode* inputs determine how the governor algorithm is to operate. With *Auto=0* governor operation is disabled and the control signal is set to the value of *Uman* unconditionally. With *Auto=1*, the governor algorithm is active and operates in either the on-line or off-line operating modes depending upon the value of the *Mode* input. *Mode*

follows the position of the generator breaker: *Mode =1* when the breaker is closed and *Mode=0* when the breaker is open.

For the off-line mode of operation Equations (3.11) and (3.12) are implemented within the PLC using the following control logic:

```
(* Compute controller states *)
dg0:=dg1*EXP_REAL(-Ts/Fm.T)+(g0-g1);
if0:=(Ts/2.0)*(fe0+fe1);
:
```

The transient droop signal *dg0*, is computed based upon the past value *dg1*, the sampling rate *Ts*, reset time *Fm.T* and the present and past gate positions *g0* and *g1* derived from the input *G*. The integral of the frequency error in the last sampling period *if0* is a function of the sampling rate *Ts*, and the present and past frequency error *fe0* and *fe1* derived from the inputs *Fsp* and *F*.

Before the control action is computed a number limit checks are performed. First are checks to see if the gate position is greater than the maximum allowable gate opening *Fm.Gmax*. If it is, then the integral action is blocked unless it is building in a negative direction. Likewise, if gate actuator control signal *uf* is positive calling for more gate opening then it too is set to zero. Also if the gates have gone beyond the maximum permissible opening than *uf* is augmented with a negatively directed value to attempt to bring the gates within operating range. The computation of *uf* includes an external speed signal *Spd*, that is equivalent to δ in the block diagram, the PI proportional gain and integral gains *Fm.P* and *Fm.I*, and the permanent and transient droop *Fm.Rd* and *Fm.Rt*. A similar check is also performed on the lower gate limit *Fm.Gmin*. Limiting the gate travel between maximum and minimum values is important particularly in the off-line mode of operation where instability may result if the gates are allowed to close too far.

```
(* check maximum gate limit against the gate position *)
IF (g0 > Fm.Gmax) THEN
        (* Block Integrator *)
        IF (if0*Fm.I) > 0.0 THEN
                if0:=0.0;
        END_IF;

        (* Compute control action and check direction *)
        uf:=Spd + fe0 + fe0*Fm.P + (if1+if0)*Fm.I - g0*Fm.Rd - dg0*Fm.Rt;
        IF uf > 0.0 THEN
                uf:=0.0;
        END_IF;

        (* Force gate in negative direction *)
        IF NOT(Fm.Gmax >= 100.0) THEN
                uf:=uf+Umin*(g0-Fm.Gmax)/(100.0-Fm.Gmax);
        END_IF;

(* check the minimum gate limit against the gate position *)
ELSIF (g0 < Fm.Gmin) THEN
        (* Block Integrator *)
        IF (if0*Fm.I) < 0.0 THEN
                if0:=0.0;
        END_IF;

        (* Compute control action and check direction *)
        uf:=Spd + fe0 + fe0*Fm.P + (if1+if0)*Fm.I - g0*Fm.Rd - dg0*Fm.Rt;
        IF uf < 0.0 THEN
```

```
            uf:=0.0;
        END_IF;

        (* Force gate in positive direction *)
        IF NOT(Fm.GMin <= 0.0) THEN
            uf:=uf+Umax*(Fm.Gmin-g0)/(Fm.Gmin);
        END_IF;

(* gates are within operating range *)
ELSE

        (* gates are within the specified limits so compute  *)
        (* the appropriate control action                    *)
        uf:=Spd + fe0 + fe0*Fm.P + (if1+if0)*Fm.I - g0*Fm.Rd - dg0*Fm.Rt;
END_IF;
```

Limit checking is also performed on the control action, and like the gate limits, the integral action on the frequency error is blocked if the control signal is saturated *uf>Umax* or *uf<Umin* , and the integral action is building in the same direction.

```
(* Check the control action against Umax/Umin *)
IF uf > Umax THEN
        uf:=Umax;
        IF (if0*Fm.I) > 0.0 THEN
            if0:=0.0;
        END_IF;

ELSIF uf < Umin THEN
        uf:=Umin;
        IF (if0*Fm.I) < 0.0 THEN
            if0:=0.0;
        END_IF;
END_IF;
:
```

The algorithm states are initialized whenever the on-line mode of operation is enabled, under the assumption of steady state conditions. Likewise the integral state is precharged with a value that results in a bumpless transfer as long as the gain Fm.I is not zero.

```
g1:=g0;
dg1:=0.0;
fe1:=0.0;

IF (Fm.I = 0.0) THEN
        if1:=0.0;
ELSE
        if1:=(g0*Fm.Rd - fe0 - Spd - fe0*Fm.P)/Fm.I;
END_IF;
:
```

At the end of the algorithm execution, the states are updated in the following manner:

```
(* Update the states for the next iteration *)
f1:=f0;         g1:=g0;
fe1:=fe0;       ge1:=ge0;
if1:=if1+if0;
dg1:=dg0;
U=uf;
:
```

Logic for the online mode of operation is much the same except *fe0* and *fe1* are replaced with *ge0* and *ge1* for the gate position error, and the feedback gains become *Gm.P* and

Gm.I for the gate PI control, *Gm.Rd* and *Gm.Rt* for the permanent and transient droop settings, and *Gm.T* is the reset time.

Variable Initialization:

```
g1:=g0;
dg1:=0.0;
ge1:=0.0;

IF (Gm.I = 0.0) THEN
        ig1:=0.0;
ELSE
        ig1:=(g0*Gm.Rd - fe0 - Spd - ge0*Gm.P)/Gm.I;
END_IF;
:
```

Compute updates for the transient droop state and integral of the gate error:

```
(* Compute controller states *)
dg0:=dg1*EXP_REAL(-Ts/Gm.T)+(g0-g1);
ig0:=(Ts/2.0)*(ge0+ge1);
:
```

Check maximum and minimum gate limits:

```
(* check maximum gate limit against the gate position *)
IF (g0 > Gm.Gmax) THEN
        (* Block Integrator *)
        IF (ig0*Gm.I) > 0.0 THEN
                ig0:=0.0;
        END_IF;

        (* Compute control action and check direction *)
        ug:=Spd + fe0 + ge0*Gm.P + (ig1+ig0)*Gm.I - g0*Gm.Rd - dg0*Gm.Rt;
        IF ug > 0.0 THEN
                ug:=0.0;
        END_IF;

        (* Force gate in negative direction *)
        IF NOT(Gm.Gmax >= 100.0) THEN
                ug:=ug + Umin*(g0-Gm.Gmax)/(100.0-Gm.Gmax);
        END_IF;

(* check the minimum gate limit against the gate position *)
ELSIF (g0 < Gm.Gmin) THEN
        (* Block Integrator *)
        IF (ig0*Gm.I) < 0.0 THEN
                ig0:=0.0;
        END_IF;

        (* Compute control action and check direction *)
        ug:=Spd + fe0 + ge0*Gm.P + (ig1+ig0)*Gm.I - g0*Gm.Rd - dg0*Gm.Rt;
        IF ug < 0.0 THEN
                ug:=0.0;
        END_IF;

        (* Force gate in positive direction *)
        IF NOT(Gm.GMin <= 0.0) THEN
                ug:=ug + Umax*(Gm.Gmin-g0)/(Gm.Gmin);
        END_IF;

(* gates are within operating range *)
ELSE

        (* gates are within the specified limits so compute *)
        (* the appropriate control action                   *)
        ug:=Spd + fe0 + ge0*Gm.P + (ig1+ig0)*Gm.I - g0*Gm.Rd - dg0*Gm.Rt;

END_IF;
```

Check for control signal saturation:

```
(* Check the control action against Umax/Umin *)
IF ug > Umax THEN
       ug:=Umax;
       IF (ig0*Gm.I) > 0.0 THEN
              ig0:=0.0;
       END_IF;

ELSIF ug < Umin THEN
       ug:=Umin;
       IF (ig0*Gm.I) < 0.0 THEN
              ig0:=0.0;
       END_IF;
END_IF;
:
```

Update the algorithm states for the next scan cycle:

```
(* Update the states for the next iteration *)
f1:=f0;                          g1:=g0;
fe1:=fe0;                        ge1:=ge0;
ig1:=ig1+ig0;
dg1:=dg0;
U=ug;
```

The disabling of the gate setpoint control loop is done external to the governor control algorithm, and is accomplished by disabling the gate setpoint ramp limiter and replacing the gate setpoint with the present gate position. In doing this, the loop is taken off line in a bumpless manner since the integral state holds its present value, and the operator's last setpoint is replaced with the present gate position when the loop is reestablished.

The algorithm code was found to run at a sampling rate of 0.025 seconds on average, under worst case conditions. However, to ensure that future code additions do not unduly affect the algorithm operation, and to make the program code more portable to other CPU's, a fixed frequency counter provided by the CPU was used to continuously track the sampling rate and update the variable *Ts* every 10 scan cycles.

For this specific application with the sampling rate given, the effects of aliasing occur at a frequency that is much higher than the generator and turbine dynamics. And because the discrete time Equations (3.11) and (3.12) have been chosen to behave as continuous time dynamics given in Figure 3-1, one may apply either discrete or continuous time design principles when selecting feedback gains.

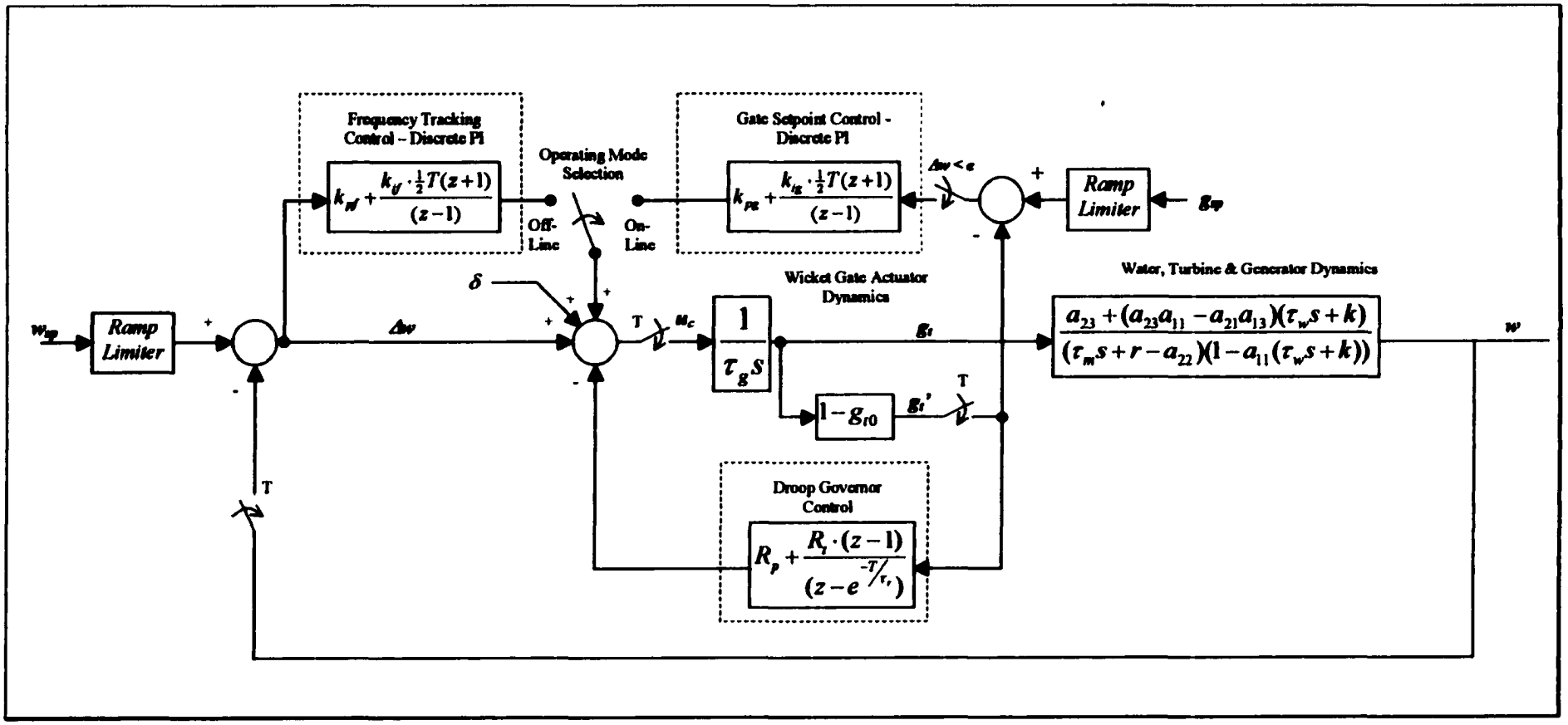

Figure 3-5 Governor Control System

3.5 Selection of Governor Settings

The governor system of Figure 3-5 requires 7 operating parameters. The droop control block uses the permanent droop R_p, the transient droop R_t and the reset time τ_r. while the frequency tracking and gate control PI blocks use the gains K_{pf}, K_{if} and K_{pg}, K_{ig} respectively.

The task of selecting each of these values can be broken down into three control problems:

1. Select values for R_p, R_t, τ_r and K_{pf}, K_{if} to provide stable speed regulation and steady state tracking of the power system frequency while off-line.
2. Select values for R_p, R_t, τ_r for the online mode of operation to provide stable speed regulation of the generator, and the appropriate amount of prime mover energy dispatch when frequency errors exist.
3. Based upon the selected values of R_p, R_t, τ_r in 2 above, and the dynamics of the gate actuator alone, select values for K_{pg}, and K_{ig} to provide wicket gate positioning with zero steady state error.

With the stability analysis of Section 3.2, some of the complexity in parameter selection may be reduced since the off-line and on-line modes of operation share a common stability region. The parameter values for R_t, and τ_r in steps 1 and 2 above may be chosen the same provided that the values fall within this region, and that K_{pf} is used to reverse the sign on Δw while operating in the off-line mode. Likewise, because the permanent droop parameter is dictated by the power system utility [16] and will have no ill effects on stability between on-line and off-line operating modes, it too may be chosen the same for steps 1 and 2.

It is necessary to select R_p=*4.0%* based upon the Ontario Hydro's specifications as outlined in [16], then choose R_t, and τ_r based upon the tuning methods of [9,4]. Setting the parameter K_{pf} = *-2.0* effectively reverses the sign on Δw, and stabilizes the off-line operating mode. All that is required is to complete steps 1 and 2 above, is to find a suitably small value for K_{if} that achieves steady state frequency tracking within a reasonable time.

Step 3 is relatively straightforward: Given the values of R_p, R_t, and τ_r, in 2, and the gate actuator dynamics, choose values for K_{pg}, and K_{ig} that provide stable gate position control. Although this loop operates while the generator is on-line, the dynamics of the generator and interconnected power system need not be considered since the frequency error is assumed to be zero at all times. When this is not the case the loop is intentionally disabled.

An algorithm that is particularly useful for tuning all of the unknown parameters of the governor is presented in Reference [19]. It uses a gradient search to minimize the quadratic cost function:

$$J = \sum_{n=0}^{\infty} y_n^T Q y_n + u_n^T R u_n \tag{3.13}$$

for a sampled data system defined by the linear matrix equations:

$$x_{n+1} = A \cdot x_n + B \cdot u_n \tag{3.14}$$
$$y_n = C \cdot x_n + D \cdot u_n$$

and the static output feedback law:

$$u_n = k y_n \tag{3.15}$$

Q and R are weighting matrices that may be arbitrarily assigned on the system inputs and outputs to achieve a "pleasing" closed loop system response. Q must be positive semi-definite and R must be positive definite.

The cost function of Equation (3.13) is minimized if values for the matrices P, k and L can be found that satisfies the following set of linear matrix equations:

$$(A + Bk'C)^T P(A + Bk'C) + C^T QC + C^T k'^T (D^T QD + R)k'C - P = 0 \tag{3.16}$$
$$(A + Bk'C)L(A + Bk'C)^T + I - L = 0 \tag{3.17}$$
$$B^T P^T ALC^T + B^T PAL^T C^T + (B^T PB + D^T QD + R)k'(CLC^T + CL^T C^T) = 0 \tag{3.18}$$
$$k = k'(I + Dk')^{-1} \tag{3.19}$$

A numerical procedure for doing this follows:

1. Choose a starting k that stabilizes the process (A, B, C, D) and compute $k'=(I-kD)^{-1}k$ from (3.19).
2. Solve the discrete Lyapunov equation (3.16) for the matrix P.
3. Solve the discrete Lyapunov equation (3.17) for the matrix L.
4. From Equation (3.18) compute:

$$\Delta k' = -(B^T PB + D^T QD + R)^{-1}(B^T P^T ALC^T + B^T PAL^T C^T)(CLC^T + CL^T C^T)^{-1} - k'$$

5. Compute a new k' based upon $k'=k'+\alpha\Delta k'$ for $0 < \alpha \leq 1.0$. Note that the value of α must be chosen so that $(A+Bk'C)$ remains stable and the trace of the matrix P is reduced at every iteration.
6. Repeat steps 2 through 5 until $\Delta k'$ diminishes to an insignificantly small value.
7. Compute the feedback gain $k=k'(I+Dk')^{-1}$ from (3.19).

To guarantee a unique solution to the Lyapunov equations, no two eigenvalues of $(A+Bk'C)$ may have the relationship $\lambda_i = 1/\lambda_j$. This condition will always be met if k' is chosen at each iteration to make $(A+Bk'C)$ asymptotically stable, or stable with at most one eigenvalue lying on the unit circle . Under these conditions both P and L will be positive definite.

Static output feedback algorithms of this type are particularly useful for solving a number of general control problems involving incomplete state variable information. [20] provides a survey of published work on the output feedback problem, including the algorithm of [19]. The algorithm of [19] and others presented in [20], if convergent, only guarantee a local minimum for J that is dependent on the initial choice of gain vector k.

To proceed with the task at hand, the system transfer function of Equation (2.24) may be represented in state space form as:

$$\dot{x} = A \cdot x + B \cdot u_c \tag{3.20}$$

With the system matrices defined as:

$$A = \begin{bmatrix} 0 & 0 & 0 \\ \dfrac{(a_{23} + a_{23}a_{11}k - a_{21}a_{13}k)}{a_{11}\tau_w} & \dfrac{(a_{11}a_{22}\tau_w/\tau_m - a_{11}k - 1)}{a_{11}\tau_w} & \dfrac{(a_{22} + a_{11}a_{22}k - a_{11}a_{22}r\tau_w/\tau_m)}{a_{11}\tau_w} \\ 0 & \dfrac{1}{\tau_m} & \dfrac{-r}{\tau_m} \end{bmatrix}$$

$$B = 60 \cdot \begin{bmatrix} \dfrac{1}{\tau_g} & \dfrac{(a_{23}a_{11} - a_{21}a_{13})}{a_{11}\tau_g} & 0 \end{bmatrix}^T$$

And the state vector:

$$x = \begin{bmatrix} g_t(t) & m(t) & w(t) \end{bmatrix}^T$$

Matrices A and B form a coupled system of first order differential equations, with $\dot{x}$ representing the first derivative of the state vector x with respect to time. The factor of 60 introduced into the B matrix is to account for the direct frequency input discussed in Section 3.2. The superscript 'T' on matrices and vectors represents the transpose operator.

The continuous time representation of Equation (3.20) may be converted to a discrete time format given by Equation (3.21) using the standard zero-order-hold transformation [15]:

$$x_{n+1} = F \cdot x_n + G \cdot u_n \tag{3.21}$$

$$F = e^{AT}$$
$$G = \int_0^T e^{A(T-\tau)} B \cdot d\tau$$

With suitable choices of matrices M_1 and M_2, the state space system of Equation (3.21) may be augmented to include the dynamics of the transient droop compensation and one of the integrators from either PI loop:

$$F_1 = \begin{bmatrix} F & \vec{0} & \vec{0} \\ (M_1 F - M_1) & e^{\frac{-T}{\tau_r}} & 0 \\ \frac{-T}{2}(M_2 F + M_2) & 0 & 1 \end{bmatrix}$$

$$G_1 = \begin{bmatrix} G & M_1 G & \frac{-T}{2} M_2 G \end{bmatrix}^T$$

With:

$$x_{1n} = \begin{bmatrix} x_n & d_n & i_n \end{bmatrix}^T$$

The state d_n represents the output from the transient droop compensation before it is scaled by R_t, and the state i_n is one of the integrator states before application of the gain k_{if} or k_{ig}.

The augmented system can be used in the cost minimization algorithm using the following state space representation:

$$x_{1n+1} = (F_1 + G_1 \cdot k_1 C_1) \cdot x_{1n} + G_1 \cdot u_n \qquad (3.22)$$
$$u_n = k_2 C_2 x_{1n}$$

The vector k_1 contains the values of known governor system control variables, while k_2 contains the control gains to be obtained by cost minimization. The matrices C_1 and C_2 are made up of constants that form the structure of the output feedback law.

For Problem 1 above, with R_p=4% and K_{pf} =-2 the following matrix selections allow the computation of R_t and k_{if}.

$$M_1 = \begin{bmatrix} 0.9 & 0 & 0 \end{bmatrix}$$
$$M_2 = \begin{bmatrix} 0 & 0 & 1 \end{bmatrix}$$

$$k_1C_1 = \begin{bmatrix} R_p & k_{pf} & 1 \end{bmatrix} \cdot \begin{bmatrix} -0.9 & 0 & 0 & 0 & 0 \\ 0 & 0 & -1 & 0 & 0 \\ 0 & 0 & -1 & 0 & 0 \end{bmatrix}$$

$$k_2C_2 = \begin{bmatrix} R_t & k_{if} \end{bmatrix} \cdot \begin{bmatrix} 0 & 0 & 0 & -1 & 0 \\ 0 & 0 & 0 & 0 & 1 \end{bmatrix}$$

Or alternately, the tuning rules provided by [9] may be used to obtain R_t directly so that only the variable k_{if} needs to be computed.

$$k_1C_1 = \begin{bmatrix} R_p & R_t & k_{pf} & 1 \end{bmatrix} \cdot \begin{bmatrix} -0.9 & 0 & 0 & 0 & 0 \\ 0 & 0 & 0 & -1 & 0 \\ 0 & 0 & -1 & 0 & 0 \\ 0 & 0 & -1 & 0 & 0 \end{bmatrix}$$

$$k_2C_2 = k_{if} \cdot \begin{bmatrix} 0 & 0 & 0 & 0 & 1 \end{bmatrix}$$

To solve Problem 2 above, the augmentation of an integrator state is not necessary and the matrices F_1 and G_1 may be simplified somewhat.

$$F_1 = \begin{bmatrix} F & \vec{0} \\ (M_1F - M_1) & e^{\frac{-T}{\tau_r}} \end{bmatrix}$$

$$G_1 = \begin{bmatrix} G & M_1G \end{bmatrix}^T$$

$$x_{1n} = \begin{bmatrix} x_n & d_n \end{bmatrix}^T$$

$$M_1 = \begin{bmatrix} 0.9 & 0 & 0 \end{bmatrix}$$

In fact cost minimization may be eliminated completely if the tuning rules of [9] are applied with R_p=4%, otherwise the parameter R_t may be obtained by choosing k_1C_1 and k_2C_2 as follows:

$$k_1C_1 = \begin{bmatrix} R_p & 1 \end{bmatrix} \cdot \begin{bmatrix} -0.9 & 0 & 0 & 0 \\ 0 & 0 & -1 & 0 \end{bmatrix}$$

$$k_2C_2 = \begin{bmatrix} R_t \end{bmatrix} \cdot \begin{bmatrix} 0 & 0 & 0 & -1 \end{bmatrix}$$

To solve Problem 3, the values for M_1, M_2, k_1C_1 and k_2C_2 are:

$$M_1 = [0.9 \quad 0 \quad 0]$$
$$M_2 = [-0.9 \quad 0 \quad 0]$$

$$k_1C_1 = [R_p \quad R_t] \cdot \begin{bmatrix} -0.9 & 0 & 0 & 0 & 0 \\ 0 & 0 & 0 & -1 & 0 \end{bmatrix}$$

$$k_2C_2 = [k_{pg} \quad k_{ig}] \cdot \begin{bmatrix} -0.9 & 0 & 0 & 0 & 0 \\ 0 & 0 & 0 & 0 & -1 \end{bmatrix}$$

The effects of frequency error are neglected by choice of C_1, while M_2 augments the matrix F_1 with the gate integrator dynamics.

The governor parameters used for each of the generators are summarized in Table 3-1. In all cases τ_r was chosen as $4\tau_w$ as per the recommendations of [9]. For the off-Line mode of operation R_t was selected based upon the tuning rules of [9], since the cost minimization resulted in slightly longer settling times. For the on-line mode, R_t was selected based upon the results of the cost minimization because it offered the same settling time with less oscillation. K_{pf} has been selected as -2 in the off-line operating mode for all generators to provide a sign reversal necessary to achieve stability.

Table 3-1 Summary of Computed Governor Settings

Generator & Control Modes	Q (diagonal elements)	R	R_p (%pu)	R_t (%pu)	T_r (sec)	k_{pf} (pu)	k_{if} (pu)	k_{pg} (pu)	K_{ig} (pu)
G1-G3 Off-Line*	0.008	1	4.0	15.0	5.0	-2.0	-0.030	-	-
G1-G3 Off-Line+	[4.0, 1.0]	0.001	4.0	11.4	5.0	-2.0	-0.025	-	-
G1-G3 On-Line	0.005	1	4.0	19.7	5.0	-	-	-	-
G1-G3 Gate Control	[2, 0.001]	350	4.0	19.7	5.0	-	-	0.088	0.0021
G4 Off-Line*	0.008	1	4.0	10.0	4.0	-2.0	-0.026	-	-
G4 Off-Line+	[4.0, 1.0]	0.001	4.0	7.5	4.0	-2.0	-0.022	-	-
G4 On-line	0.005	1	4.0	11.5	4.0	-	-	-	-
G4 Gate Control	[2, 0.001]	350	4.0	11.5	4.0	-	-	0.073	0.0020

* Transient droop computed based upon Reference [9] – settings applied to generator.
+ Transient droop computed based upon Cost minimization – settings not applied to generator.

3.6 Experimental Results

Figure 3-6 shows a frequency disturbance response for Generator 1 operating in the Off-Line mode. The disturbance was created by injecting a signal of 1.0 at the δ input shown in Figure 3-5. The traces shown in red are the actual responses measured at the PLC inputs, the trace shown in green is the predicted generator response based on the model presented in Chapter 2 and the applied governor settings. The remaining blue trace is the predicted response of the generator had the transient droop been tuned with the cost minimization algorithm. As can be seen from the figure, the settling time is achieved in approximately 100 seconds, and the PI frequency-tracking block provides good steady state tracking.

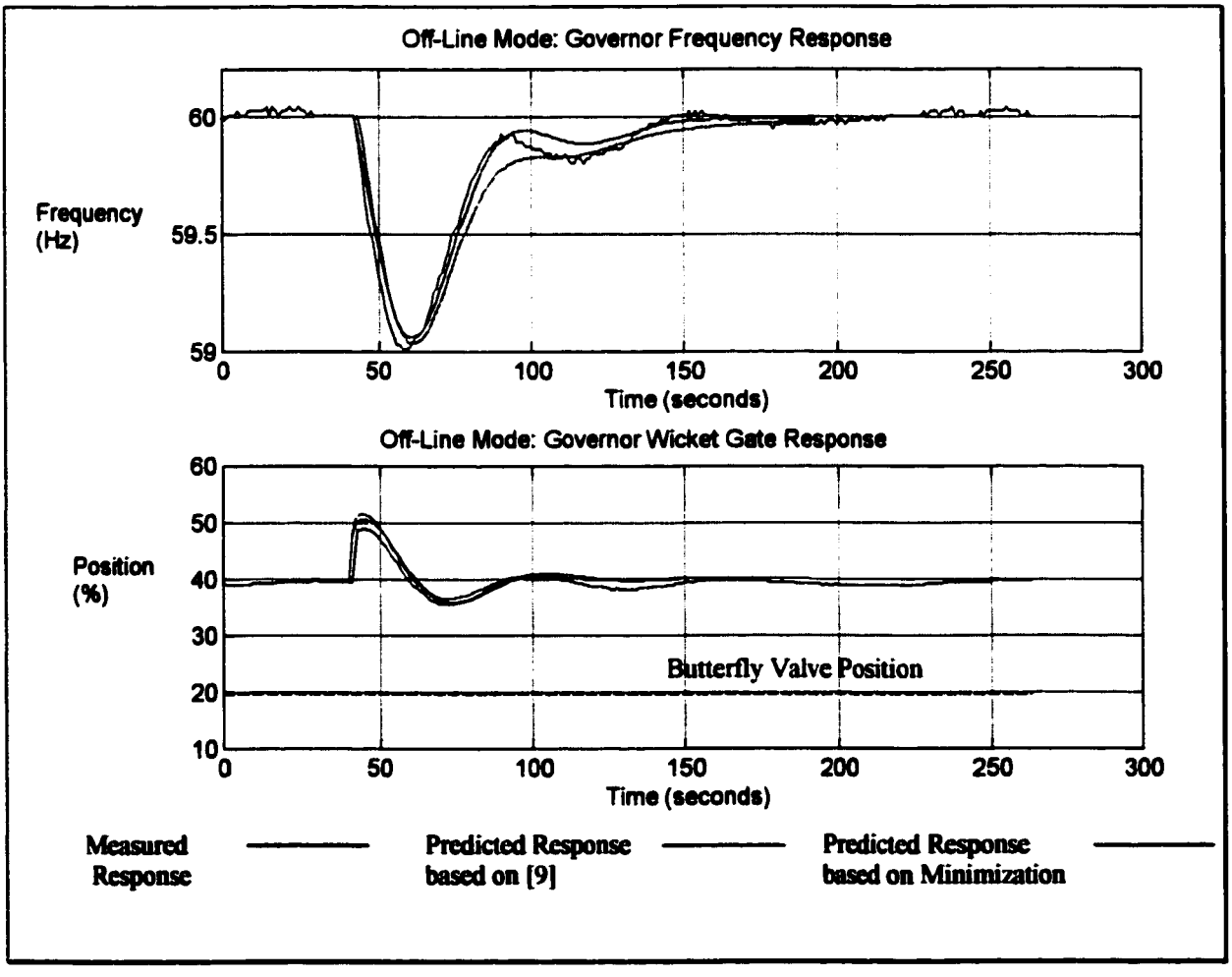

Figure 3-6 Generator 1 Off-Line Disturbance Response

Figure 3-7 shows the simulated disturbance response of Generator 1 operating in the on-line mode. The simulation was done with a signal of 1.0 was injected at the δ input shown in Figure 3-5, and the model developed in Chapter 2 without additional power system dynamics. The red trace is for governor settings based upon the tuning rules of Reference [9], while the green trace is for R_t computed with the cost minimization algorithm of the previous section. The second set of settings were applied to the generators given that the setting times are approximately the same, but with less oscillation resulting from the cost minimization method.

No actual responses for the generator are available, since power system disturbances occur infrequently and cannot be created artificially.

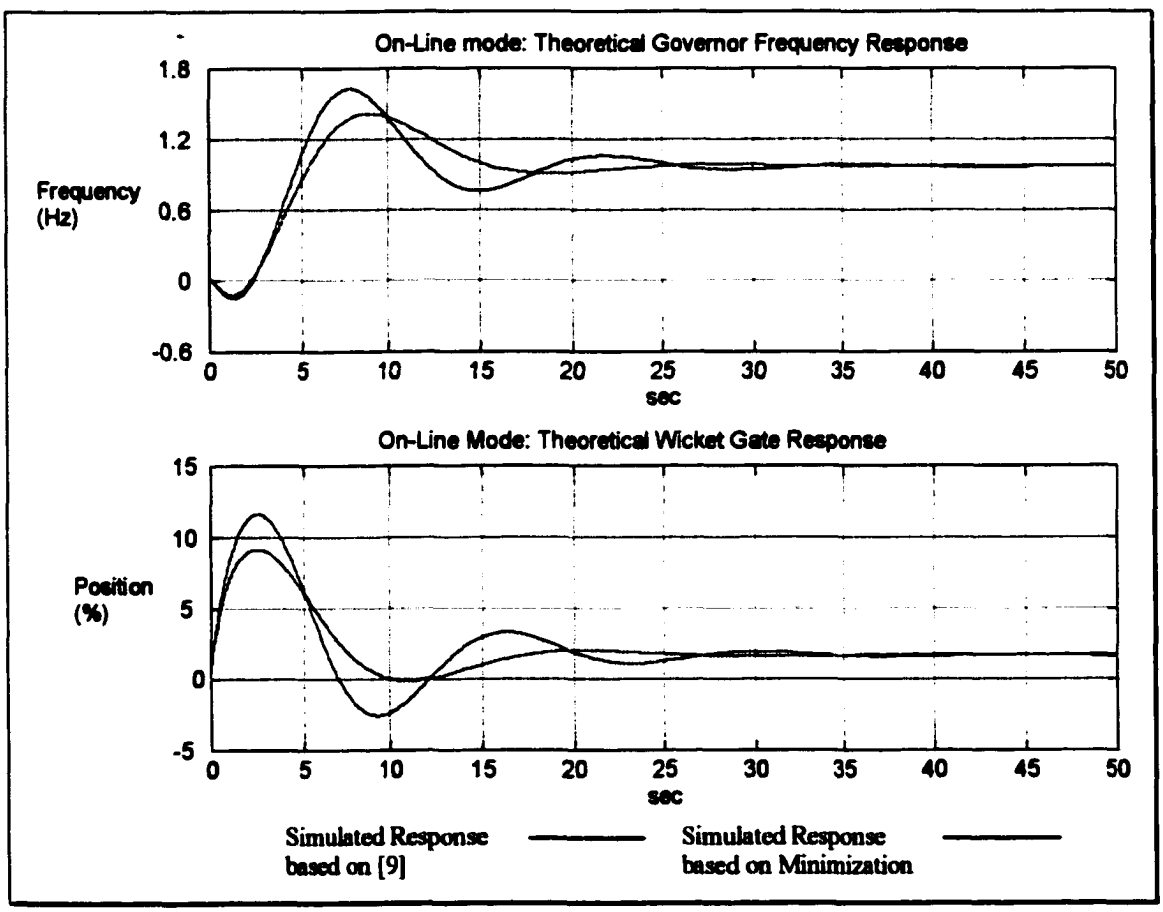

Figure 3-7 Generator 1 Simulated On-Line Disturbance Response

Figure 3-8 shows the actual and predicted wicket gate response for Generator 1, with the ramp limiter of Figure 3-5 disabled. Steady state tracking of the desired wicket gate setpoint is achieved with the PI controller. The overshoot did not create any practical problems, and was masked for the most part by the ramp limiter that acted on the setpoint.

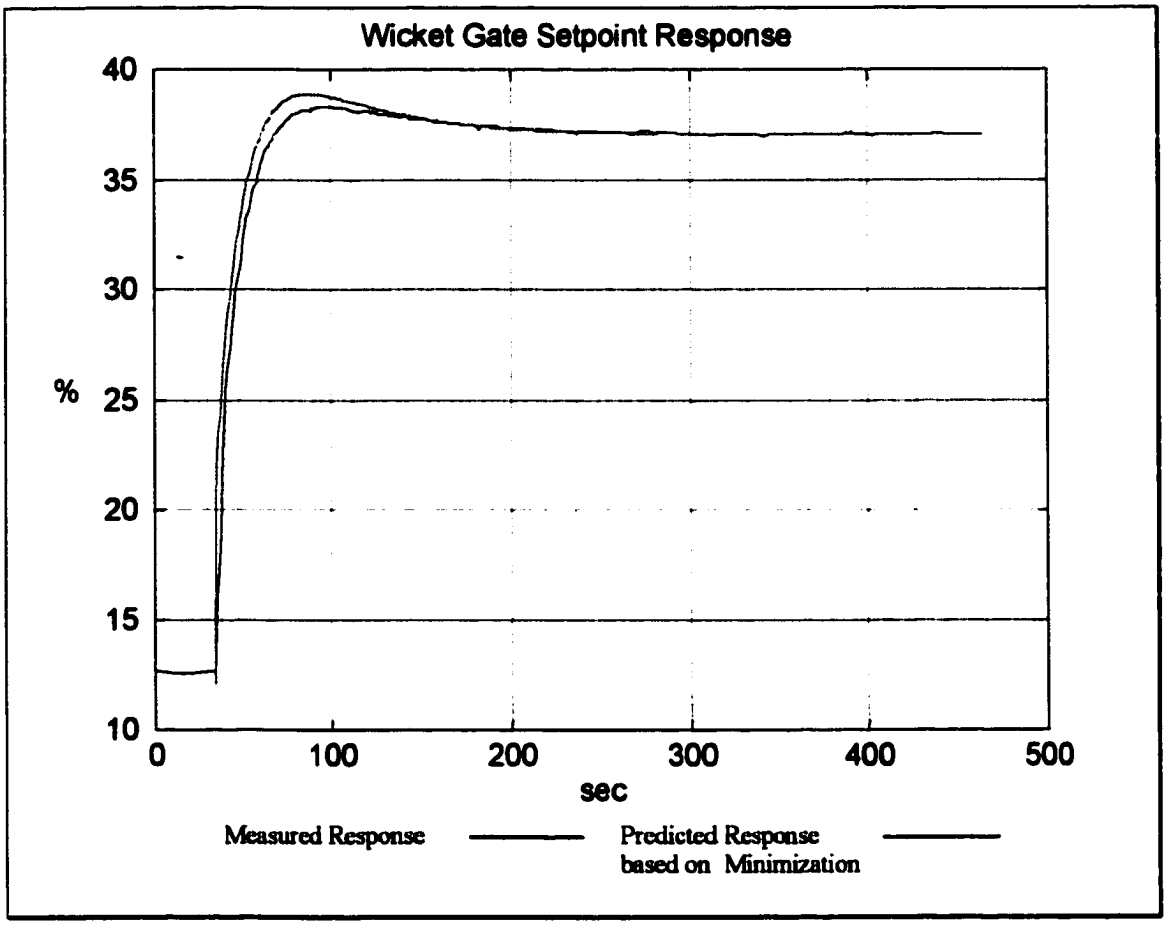

Figure 3-8 Generator 1 Wicket Gate Setpoint Response

Figures 3-9 and 3-10 show a complete startup and shutdown sequence for generator 1. At startup the butterfly valve is opened to the throttled position $\approx 20\%$, in preparation for the governor control to be initiated in the off-line mode of operation. With the partial butterfly valve opening and the wicket gate leakage alone, the generator shaft receives enough torque to begin accelerating toward synchronous speed. Shortly after the butterfly has come to rest, the governor is enabled and the wicket gates immediately travel into the stable operating range of the inverse turbine characteristic $g_t > 20\%$. The governor's frequency setpoint is set to that of the power system with ramp limiting of 0.25 Hz/ sec. In approximately 300 seconds the governor has locked on the power system frequency, and the phase angle slip-rate is slow enough allow synchronizing. When the unit breaker closes the butterfly valve is forced to the fully open position, and the governor algorithm

immediately switches to the on-line mode of operation. Likewise, the gate control PI loop is enabled with an initial setpoint *10%*, until commanded to do otherwise by the plant operator.

The shutdown sequence is similar. The butterfly valve is closed to the throttled position *≈20%*, in preparation for a breaker open signal. Upon a breaker trip, the governor algorithm switches to the off-line mode of operation, and the wicket gates immediately travel into the stable operating range of the inverse turbine characteristic. The generator frequency deviates a small amount as the gates adjust to compensate for the disturbance that is created when the breaker is opened. The generator remains at rated speed tracking the power system frequency until commanded to stop by a plant operator. When the stop signal occurs, both the wicket gates and the butterfly valve are forced to the closed position and the governor control is disabled.

Similar results to those presented above were obtained for the other units. Due to the increased mechanical time-constant and wicket gate time-constant of Generator 4, the settling times for the various operating modes were found to be slightly greater than that of Generators 1, 2 and 3.

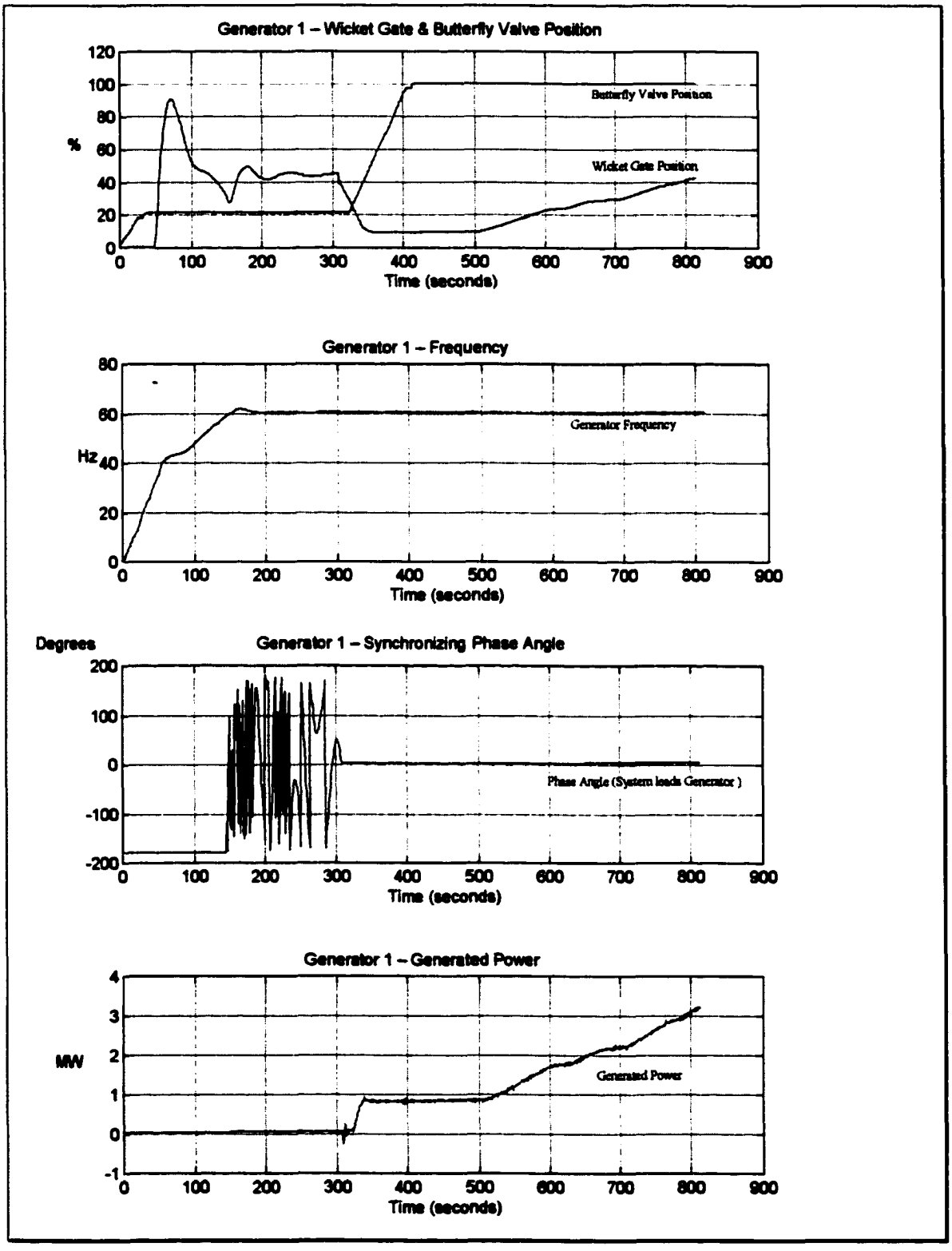

Figure 3-9 Generator 1 Startup Sequence

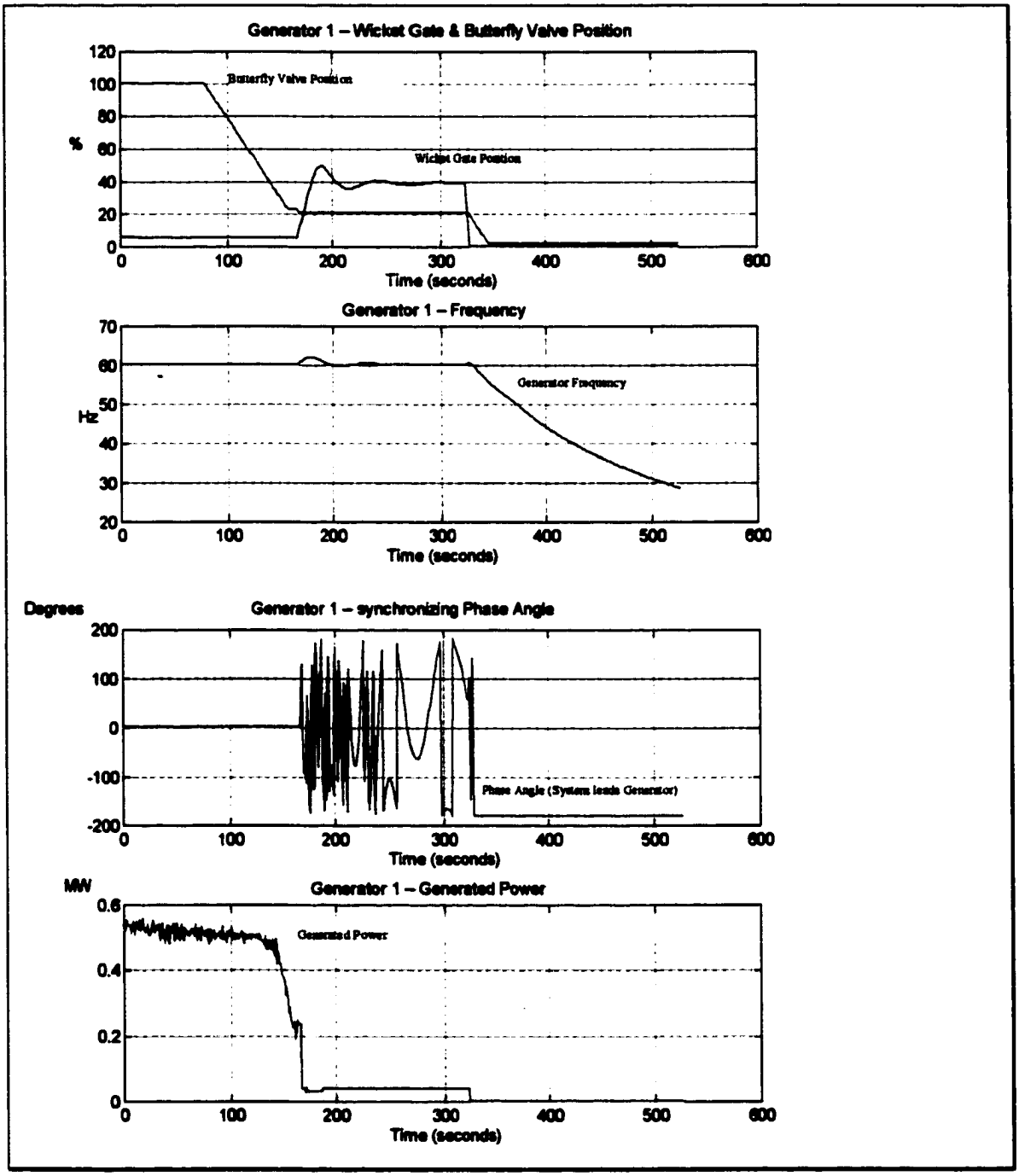

Figure 3-10 Generator 1 Shutdown Sequence

Chapter 4

Future Work

The modeling and governor design presented in this thesis meets all of the design objectives set out in Chapter 1 and has been successfully implemented at the plant. At the time of this writing, the algorithm has been in successful operation for a period of eight months. The governor has served the plant far better than the previous means of control by providing quick generator startup, synchronization, and reliable operation.

The cost minimization algorithm presented in chapter 3 converged well for the problem at hand and provided inherently stable and robust solutions. However, the need to supply an initial stabilizing gain vector, and lack of correlation between the Q and R matrices and any practical design objectives begs one to seek out better methods of tuning.

Future efforts might be best directed towards expanding on the work of Hovey [9] to develop a generalized stability region and tuning parameters based not only on the generator time constansts, but also on a full set of turbine constants a_{11}-a_{23}. The frequency tracking PI block given proved to be very useful for synchronization, and so its control gains might also be considered in any development of a generalized set of tuning rules.

Bibliography

1. Streeter, Victor L., Wylie, E. Benjamin, "Fluid Mechanics", McGraw-Hill Book Company, New York, 1979.
2. Oldenburger, R., Donelson, Jr. J., "Dynamic Response of a Hydroelectric Plant", AIEE Transactions, Vol. 81, Pt III, pp. 403-418, 1962.
3. IEEE Committee Report, "Dynamic Models for Steam and Hydro Turbines in Power System Studies", IEEE Transactions Vol. PAS-92, pp.1904-1915, 1973.
4. Working Group on Prime Mover and Energy Supply Models for System Dynamic Performance Studies, "Hydraulic Turbine and Turbine Control Models for System Dynamic Studies", IEEE Transactions on Power systems, Vol. 7, No. 1, 1992.
5. Woodward, J. L. "Hydraulic Turbine Transfer Function for use in Governor Studies", IEE Proc., Vol. 115, No. 3, 1968.
6. Trudnowski, D. J., Agee J. C., "Identifying a Hydraulic Turbine Model from Measured Field Data", IEEE Transactions on Energy Conversion, Vol. 10, No. 4, 1995.
7. Vournas, C. D., Papaioannou, G., "Modeling and Stability of a Hydro Plant with Two Surge Tanks", IEEE Transactions on Energy Conversion, Vol. 10, No. 2, 1995.
8. Shinskey, F.G. "Process Control Systems – Application, Design, and Tuning", Third Edition, McGraw-Hill Book Company, New York, 1988.
9. Hovey, L. M. "Optimum Adjustment of Hydro Governors on Manatoba Hydro System", AIEE Trans. Vol 81, Part III, Dec. 1962.
10. Hagihara, S., Yokota, K., Goda, K., Isobe, K., "Stability of a hydraulic turbine generating unit controlled by PID governor", IEEE Trans. Power Apparatus and Systems, Vol. PAS-98, No. 6, 1979.
11. Orelind, G., Wozniak, L., Medanic, J., Whittemore, T., "Optimal PID gain schedule for hydrogenerators – design and applications" IEEE Trans. on Energy Conversion, Vol. 4, No. 3, Sept. 1989.
12. Findlay, D., Davie, H., Foord, T. R., Marshall, A.G., Winning, D.J., "Microprocessor based adaptive water turbine governor", IEE Proc. Vol. 127, Part C, No. 6, Nov. 1980.
13. Malik, O. P., Zeng, Y., "Design of a robust adaptive controller for a water turbine governing system" IEEE Trans. on Energy Conversion, Vol. 10, No. 2, June 1995.
14. Jiang, J. "Design of an optimal robust governor for hydraulic turbine generating units" IEEE Trans. on Energy Conversion, Vol. 10, No. 1, March 1995.
15. Belanger, P. R. "Control Engineering: A modern approach", Saunders College Publishing, 1995.
16. Bayne, J.P. "Governor Settings in the Northwest Region" Ontario Hydro Research Division Report 77-118-H, March 1977.

17. Ontario Hydro, "Operating Hydraulic Data for Kakabeka Falls GS", Regional Trades and Operating Information System Technical Directive HO-911-R1, September 1983.

18. Hostetter, G.H., Savant, C.J., Stefani, R.T., "Design of Feedback Control Systems", Holt, Rinehart and Wilson, New York, 1982.

19. Moerder, D., Calise, A., "Convergence of a Numerical Algorithm for Calculating Optimal Output Feedback Gains", IEEE Transactions on Automatic Control, Vol. AC30, No. 9, September 1985.

20. Syrmos, V.L., Abdallah, C., Dorato, P., "Static Output feedback: A Survey", IEEE Proceedings of the 33rd Conference on Decision and Control, Lake Buena Florida, December 1994.